Heavy flavor pentaquarks with four heavy quarks

Hong-Tao An,[1,2,*] Kan Chen,[1,2,3,4,†] Zhan-Wei Liu,[1,2,5,‡] and Xiang Liu[1,2,5,§]

[1]*School of Physical Science and Technology, Lanzhou University, Lanzhou 730000, China*
[2]*Research Center for Hadron and CSR Physics, Lanzhou University and Institute of Modern Physics of CAS, Lanzhou 730000, China*
[3]*Center of High Energy Physics, Peking University, Beijing 100871, China*
[4]*School of Physics and State Key Laboratory of Nuclear Physics and Technology, Peking University, Beijing 100871, China*
[5]*Lanzhou Center for Theoretical Physics, Key Laboratory of Theoretical Physics of Gansu Province, and Frontiers Science Center for Rare Isotopes, Lanzhou University, Lanzhou 730000, China*

(Received 14 May 2021; accepted 4 June 2021; published 30 June 2021)

In this work, we carry out the study of heavy flavor pentaquarks with four heavy quarks, which have typical $QQQQ\bar{q}$ configuration. Within the chromomagnetic interaction model, the mass spectrum of these discussed $QQQQ\bar{q}$ pentaquarks is given. In addition to the mass spectrum analysis, we also illustrate their two-body strong decay behavior by estimating some ratios of decay channels. By these efforts, we suggest that a future experiment should pay attention to this kind of pentaquark.

DOI: 10.1103/PhysRevD.103.114027

I. INTRODUCTION

On March 3, 2021, LHC announced that 59 new hadrons were reported over the past decade [1]. The present situation of hadronic states is far beyond what Gell-Mann and Zweig thought possible [2–4]. Among these observed states, these P_c states existing in the $\Lambda_b \to J/\psi K^- p$ decay are good candidates of exotic molecular pentaquark [5–15]. The name *pentaquark* was first proposed in Refs. [16,17], and there were many theoretical explorations of pentaquark [18–22].

In 2003, LEPS announced the observation of $\Theta^+(1540)$ with strangeness $S = +1$ [23], which has the $uudd\bar{s}$ component. Of course, $\Theta^+(1540)$ stimulated extensive studies of pentaquark [24–27]. However, some high precision experiments such as BES [28], *BABAR* [29], Belle [30], and CDF [31] did not confirm the existence of $\Theta^+(1540)$. Facing this situation, one realized again that our understanding of nonperturbative behavior of quantum chromodynamics is still absent, which is a lesson of $\Theta^+(1540)$.

Obviously, it is not the end of the exploration of exotic hadronic matter. With the accumulation of experimental data, more and more charmoniumlike XYZ states have been discovered since 2013, which again inspired a theorist's extensive interest in investigating exotic hadronic states [32–39]. Especially, in 2015, the LHCb Collaboration measured the $\Lambda_b^0 \to J/\psi K^- p$ decay and observed two hidden-charm pentaquarklike resonances $P_c(4380)$ and $P_c(4450)$ in the $J/\psi p$ invariant mass spectrum, which indicates that they have a minimal quark content of $uudc\bar{c}$ [5,6]. In 2019, LHCb found three narrow P_c structures in the $J/\psi p$ invariant mass spectrum of $\Lambda_b \to J/\psi K^- p$ [7], where this new measurement shows that $P_c(4450)$ is actually composed of two substructures, $P_c(4440)$ and $P_c(4457)$ with 5.4σ significance. The characteristic mass spectrum of P_c provides a strong evidence for existence of hidden-charm molecular pentaquarks [11–15].

At present, searching for exotic hadronic states is still full of challenge and opportunity. As theorists, we should provide valuable prediction, which requires us to continue to find some crucial hint for exotic hadronic states.

We may borrow some idea of proposing stable tetraquark state with $QQ\bar{q}\bar{q}$ configuration. Stimulated by the observation of double charm baryon $\Xi_{cc}^{++}(3620)$ [40], Refs. [41–43] studied the possible stable tetraquark state with the $QQ\bar{q}\bar{q}$ configuration. Here, the $QQ\bar{q}\bar{q}$ configuration can be obtained by replacing light quark q of double heavy baryon QQq with $\bar{q}\bar{q}$ pair since the color structure of q and $\bar{q}\bar{q}$ can be the same. Along this line, we may continue to replace $\bar{q}$ of $QQ\bar{q}\bar{q}$ with a QQ pair and get the $QQQQ\bar{q}$ configuration, which is a typical pentaquark configuration (see Fig. 1).

As a new type of pentaquark, the $QQQQ\bar{q}$ pentaquark draws our attention to explore its mass spectrum and decay

*anht14@lzu.edu.cn
†chenk_10@pku.edu.cn
‡liuzhanwei@lzu.edu.cn
§xiangliu@lzu.edu.cn

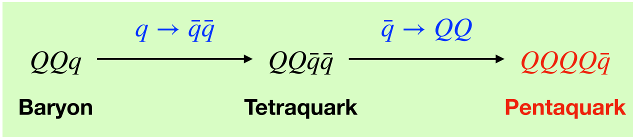

FIG. 1. Evolution of the $QQQQ\bar{q}$ pentaquark from double heavy tetraquark and baryon.

behavior. This information is valuable to future experimental search for the $QQQQ\bar{q}$ pentaquark. In this work, we systematically present the mass spectrum of the S-wave $QQQQ\bar{q}$ system within the framework of chromomagnetic interaction (CMI) model [44], which has been widely adopted to study the mass spectra of multiquark systems [41,45–62]. Moreover, in this work, we estimate the ratios of the possible decays of the $QQQQ\bar{q}$ pentaquarks, which are crucial for hunting this kind of pentaquark.

This paper is organized as follows. After introduction, the adopted CMI model will be introduced in in Sec. II. In Sec. III, we present the mass spectra of S-wave $QQQQ\bar{q}$ pentaquarks and estimate the ratios of possible strong decay widths. Finally, a short summary is followed in Sec. IV.

II. THE CHROMOMAGNETIC INTERACTION MODEL

The effective Hamiltonian involved in the estimated mass spectrum of these discussed pentaquarks

$$H = \sum_i m_i + H_{\mathrm{CMI}} = \sum_i m_i - \sum_{i<j} C_{ij} \vec{\lambda}_i \cdot \vec{\lambda}_j \vec{\sigma}_i \cdot \vec{\sigma}_j, \quad (1)$$

where m_i denotes the effective mass of the ith constituent quark when considering these effects from kinetic energy, color confinement, and so on. H_{CMI}, as the chromomagnetic interaction Hamiltonian, is composed of Pauli matrices σ_i and Gell-Mann matrices λ_i. Here, λ_i should be replaced by $-\lambda_i^*$ for antiquark, and C_{ij} denotes the effective coupling constant between the ith quark and jth quark, which depends on the quark masses and the ground particle's spatial wave function. As input, C_{ij} is fixed by the involved hadron masses.

Usually, there exists overestimate to the predicted hadron masses by Eq. (1) [41,45–55]. Additionally, the effective mass m_i in Eq. (1) does not incorporate attraction sufficiently. The mass of the pentaquark state reads as

$$M = M_{\mathrm{ref}} - \langle H_{\mathrm{CMI}} \rangle_{\mathrm{ref}} + \langle H_{\mathrm{CMI}} \rangle, \quad (2)$$

where M_{ref}, $\langle H_{\mathrm{CMI}} \rangle_{\mathrm{ref}}$, and $\langle H_{\mathrm{CMI}} \rangle$ are the physical mass of the reference system, the corresponding CMI eigenvalue, and the CMI eigenvalue for the discussed multiquark state, respectively. For M_{ref}, we can use the threshold of a reference baryon-meson system whose quark content is the same as the considered pentaquark states. For example, for the $nncc\bar{c}$ system, we can use $(M_{\Xi_{cc}} + M_D) - (\langle H_{\mathrm{CMI}} \rangle_{\Xi_{cc}} + \langle H_{\mathrm{CMI}} \rangle_D) + \langle H_{\mathrm{CMI}} \rangle_{nncc\bar{c}}$ or $(M_{\Sigma_c} + M_{J/\psi}) - (\langle H_{\mathrm{CMI}} \rangle_{\Sigma_c} + \langle H_{\mathrm{CMI}} \rangle_{J/\psi}) + \langle H_{\mathrm{CMI}} \rangle_{nncc\bar{c}}$ to obtain the mass spectra. All possible used M_{ref} values are shown in Table I.[1] With this treatment, the dynamical effects that are not incorporated in the original approach can be compensated [50]. This approach of determining the masses of pentaquark states is named as the reference mass scheme here.

TABLE I. The adopted masses of conventional hadrons for determining parameters (in units of MeV) [59,63].

Hadrons	$I(J^P)$	Mass	Hadrons	$I(J^P)$	Mass
D	$1/2(0^-)$	1869.6	D^*	$1/2(1^-)$	2010.3
D_s	$0(0^-)$	1968.3	D_s^*	$0(1^-)$	2112.2
B	$1/2(0^-)$	5279.3	B^*	$1/2(1^-)$	5324.7
B_s	$0(0^-)$	5366.8	B_s^*	$0(1^-)$	5415.4
Ξ_{cc}	$1/2(1/2^+)$	3621.4	Ξ_{cc}^*	$1/2(3/2^+)$	(3696.1)
Ω_{cc}	$0(1/2^+)$	(3731.8)	Ω_{cc}^*	$0(3/2^+)$	(3802.4)
Ξ_{cb}	$1/2(1/2^+)$	(6922.3)	Ω_{cb}	$0(1/2^+)$	(7010.7)
Ξ'_{cb}	$1/2(1/2^+)$	(6947.9)	Ω'_{cb}	$0(1/2^+)$	(7047.0)
Ξ_{cb}^*	$1/2(3/2^+)$	(6973.2)	Ω_{cb}^*	$0(3/2^+)$	(7065.7)
Ξ_{bb}	$1/2(1/2^+)$	(10168.9)	Ξ_{bb}^*	$1/2(3/2^+)$	(10188.8)
Ω_{bb}	$0(1/2^+)$	(10259.0)	Ω_{bb}^*	$0(3/2^+)$	(10267.5)
Ω_{ccc}	$0(3/2^+)$	(4785.6)	Ω_{bbb}	$0(3/2^+)$	(14309.7)
Ω_{ccb}	$0(1/2^+)$	(7990.3)	Ω_{ccb}^*	$0(3/2^+)$	(8021.8)
Ω_{bbc}	$0(1/2^+)$	(11165.0)	Ω_{bbc}^*	$0(3/2^+)$	(11196.4)

Alternatively, a color-electric term can be introduced here [27,57–61],

$$H_{\mathrm{CEI}} = -\sum_{i<j} A_{ij} \vec{\lambda}_i \cdot \vec{\lambda}_j. \quad (3)$$

With deduction

$$\sum_{i<j} (m_i^0 + m_j^0) \vec{\lambda}_i \cdot \vec{\lambda}_j = \frac{1}{2} \sum_{i,j} (m_i^0 + m_j^0) \vec{\lambda}_i \cdot \vec{\lambda}_j - \sum_i m_i^0 (\vec{\lambda}_i)^2 = \left(\sum_i m_i^0 \vec{\lambda}_i \right) \cdot \left(\sum_i \vec{\lambda}_i \right) - \frac{16}{3} \sum_i m_i^0, \quad (4)$$

where the color operator $\sum_i \vec{\lambda}_i$ nullifies any colorless physical state, we have the Hamiltonian of the modified CMI model

[1] Since some of the heavy flavor baryons are not yet observed, we adopt the theoretical results in Ref. [59] as input.

$$\begin{aligned}
H &= \sum_i m_i^0 + H_{\mathrm{CEI}} + H_{\mathrm{CMI}} \\
&= \sum_i m_i^0 - \sum_{i<j} A_{ij}\vec{\lambda}_i\cdot\vec{\lambda}_j - \sum_{i<j} v_{ij}\vec{\lambda}_i\cdot\vec{\lambda}_j\vec{\sigma}_i\cdot\vec{\sigma}_j, \\
&= -\frac{3}{4}\left(-\frac{4}{3}\sum_i m_i^0\right) - \sum_{i<j} A_{ij}\vec{\lambda}_i\cdot\vec{\lambda}_j - \sum_{i<j} v_{ij}\vec{\lambda}_i\cdot\vec{\lambda}_j\vec{\sigma}_i\cdot\vec{\sigma}_j, \\
&= -\frac{3}{4}\sum_{i<j}\left[\frac{1}{4}(m_i^0+m_j^0)+\frac{4}{3}A_{ij}\right]\vec{\lambda}_i\cdot\vec{\lambda}_j - \sum_{i<j} v_{ij}\vec{\lambda}_i\cdot\vec{\lambda}_j\vec{\sigma}_i\cdot\vec{\sigma}_j, \\
&= -\frac{3}{4}\sum_{i<j} m_{ij}V_{ij}^{\mathrm{C}} - \sum_{i<j} v_{ij}V_{ij}^{\mathrm{CMI}}. \qquad (5)
\end{aligned}$$

In the above expression, $V_{ij}^{\mathrm{C}} = \vec{\lambda}_i\cdot\vec{\lambda}_j$ and $V_{ij}^{\mathrm{CMI}} = \vec{\lambda}_i\cdot\vec{\lambda}_j\vec{\sigma}_i\cdot\vec{\sigma}_j$ denote the color and color-magnetic interactions between quarks, respectively. A new mass parameter of quark pair should be defined, i.e.,

$$m_{ij} = \frac{1}{4}(m_i^0+m_j^0)+\frac{4}{3}A_{ij}. \qquad (6)$$

By these conventional hadron masses (see Table I), we may fix the parameters m_{ij} and v_{ij} (see Table II). Interested readers can refer to Refs. [27,59–61] for more details. With this modified CMI model scheme, we can give mass spectrum of the $QQQQ\bar{q}$ pentaquarks.

When calculating the mass of the pentaquark states, we need the information of the total wave function, which is composed of space, flavor, color, and spin wave functions, i.e.,

$$\psi_{\mathrm{tot}} = \psi_{\mathrm{space}}\otimes\psi_{\mathrm{flavor}}\otimes\psi_{\mathrm{color}}\otimes\psi_{\mathrm{spin}}. \qquad (7)$$

Since we only focus on the low-lying S-wave pentaquark states, the symmetrical constraint from spatial pentaquark wave function is trivial. For the discussed $QQQQ\bar{q}$ pentaquarks, their $\psi_{\mathrm{flavor}}\otimes\psi_{\mathrm{color}}\otimes\psi_{\mathrm{spin}}$ wave functions of pentaquark states should be fully antisymmetric when exchanging identical quarks. All the possible flavor combinations for the $QQQQ\bar{q}$ pentaquark system are shown in Table III, by which we further determine $\psi_{\mathrm{flavor}}\otimes\psi_{\mathrm{color}}\otimes\psi_{\mathrm{spin}}$ wave functions, which satisfy $\{1234\}$, $\{123\}$, and $\{12\}\{34\}$ symmetry. Here, we use the notation $\{1234\}$ to label that the first, second, third, and fourth quarks have antisymmetry property, which will be applied in the following discussions. For identifying the pentaquark configuration with certain exchanging symmetry, we use the approach of Young diagram and Young tableau, which represents the irreducible bases of the permutation group.

The color wave functions for $QQQQ\bar{q}$ pentaquark system are expressed as a direct product

$$[3_c\otimes 3_c\otimes 3_c\otimes 3_c]\otimes\bar{3}_c. \qquad (8)$$

Due to the requirement of color confinement, the color wave function must be a singlet. Therefore, the four heavy quarks should be in the color triplet states, and the corresponding partition [211] reads as

$$\begin{array}{|c|c|}\hline 1 & 2 \\ \hline 3 \\ \cline{1-1} 4 \\ \cline{1-1}\end{array} = \{(12)_6\,(34)_{\bar{3}}\}_3\,, \quad \begin{array}{|c|c|}\hline 1 & 3 \\ \hline 2 \\ \cline{1-1} 4 \\ \cline{1-1}\end{array} = \{(12)_{\bar{3}}\,34\}_3\,,$$
$$\begin{array}{|c|c|}\hline 1 & 4 \\ \hline 2 \\ \cline{1-1} 3 \\ \cline{1-1}\end{array} = \{(123)_1\,4\}_3\,. \qquad (9)$$

Here, the subscript labels the irreducible representation of SU(3). Then, by combining the antitriplet from light antiquark with the deduced three color triplets in Eq. (9), we obtain the following three color singlets for all the studied pentquark systems:

$$\begin{aligned}
|C_1\rangle &= |\,[(12)_6\,(34)_{\bar{3}}]_3\,(\bar{5})_{\bar{3}}\rangle = \begin{array}{|c|c|}\hline 1 & 2 \\ \hline 3 \\ \cline{1-1} 4 \\ \cline{1-1}\end{array}_{\,3} \otimes (\bar{5})_{\bar{3}} \\
&= \frac{1}{4\sqrt{3}}\Big[(2bbgr - 2bbrg + gbrb - gbbr + bgrb - bgbr \\
&\quad - rbgb + rbbg - brgb + brbg)\bar{b} + (2rrbg - 2rrgb \\
&\quad + rgrb - rgbr + grrb - grbr + rbgr - rbrg + brgr \\
&\quad - brrg)\bar{r} + (2ggrb - 2ggbr - rggb + rgbg - grgb \\
&\quad + grbg + gbgr - gbrg + bggr - bgrg)\bar{g}\Big], \qquad (10)
\end{aligned}$$

TABLE II. Coupling parameters for the schemes in units of MeV. Here, $q = n$, s ($n = u$, d), and $Q = c$, b.

The reference mass scheme						
C_{cc}	C_{bb}	C_{cb}	$C_{c\bar{n}}$	$C_{c\bar{s}}$	$C_{b\bar{n}}$	$C_{b\bar{s}}$
3.3	1.8	2.0	6.6	6.7	2.1	2.3

The modified model CMI scheme						
m_{cc}	m_{bb}	m_{cb}	$m_{c\bar{n}}$	$m_{c\bar{s}}$	$m_{b\bar{n}}$	$m_{b\bar{s}}$
792.9	2382.4	1604.0	493.3	519.0	1328.3	1350.8
v_{cc}	v_{bb}	v_{cb}	$v_{c\bar{n}}$	$v_{c\bar{s}}$	$v_{b\bar{n}}$	$v_{b\bar{s}}$
3.5	1.9	2.0	6.6	6.7	2.1	2.3

TABLE III. All possible flavor combinations for the $QQQQ\bar{q}$ pentaquark system with $q = n$, s ($n = u$, d), and $Q = c$, b.

System	Flavor combinations				
$QQQQ\bar{q}$	$cccc\bar{n}$	$cccb\bar{n}$	$ccbb\bar{n}$	$bbbc\bar{n}$	$bbbb\bar{n}$
	$cccc\bar{s}$	$cccb\bar{s}$	$ccbb\bar{s}$	$bbbc\bar{s}$	$bbbb\bar{s}$

$$
\begin{aligned}
|C_2\rangle &= |\,[(12)_{\bar{3}}\,34]_3\,(\bar{5})_{\bar{3}}\rangle = \begin{array}{|c|c|}\hline 1 & 3 \\ \hline 2 & \multicolumn{1}{c}{} \\ \cline{1-1} 4 & \multicolumn{1}{c}{} \\ \cline{1-1}\end{array}_{\,3} \otimes (\bar{5})_{\bar{3}} \\
&= \frac{1}{12}\Big[(3bgbr - 3gbbr - 3brbg + 3rbbg - rbgb + gbrb \\
&\quad +2grbb + brgb - bgrb - 2rgbb)\bar{b} + (3grrb - 3rgrb \\
&\quad -3brrg + 3rbrg - rbgr - 2gbrr + 2bgrr - grbr \\
&\quad +rgbr + brgr)\bar{r} + (3grgb - 3rggb + 3bggr - 3gbgr \\
&\quad -grbg + rgbg + 2rbgg - 2brgg + gbrg - bgrg)\bar{g}\Big],
\end{aligned} \tag{11}
$$

and

$$
\begin{aligned}
|C_3\rangle &= |\,[(123)_1\,4]_3\,(\bar{5})_{\bar{3}}\rangle = \begin{array}{|c|c|}\hline 1 & 4 \\ \hline 2 & \multicolumn{1}{c}{} \\ \cline{1-1} 3 & \multicolumn{1}{c}{} \\ \cline{1-1}\end{array}_{\,3} \otimes (\bar{5})_{\bar{3}} \\
&= \frac{1}{3\sqrt{2}}\Big[(grbb - rgbb + rbgb - brgb + bgrb - gbrb)\bar{b} \\
&\quad +(grbr - rgbr + rbgr - brgr + bgrr - gbrr)\bar{r} \\
&\quad +(grbg - rgbg + rbgg - brgg + bgrg - gbrg)\bar{g}\Big].
\end{aligned} \tag{12}
$$

Next, we discuss the spin wave function in spin space. For the $QQQQ\bar{q}$ pentaquark system with total spin $J = 5/2$, the spin state can be represented by partition [5], i.e.,

$$
\begin{array}{|c|c|c|c|c|}\hline 1 & 2 & 3 & 4 & 5 \\ \hline\end{array}_{\,S_1}\,. \tag{13}
$$

The spin wave functions for the $QQQQ\bar{q}$ pentaquark with $J = 3/2$ are represented in partition [41] as

$$
\begin{array}{|c|c|c|c|}\hline 1 & 2 & 3 & 4 \\ \hline 5 & \multicolumn{3}{c}{} \\ \cline{1-1}\end{array}_{\,S_1},
\begin{array}{|c|c|c|c|}\hline 1 & 2 & 3 & 5 \\ \hline 4 & \multicolumn{3}{c}{} \\ \cline{1-1}\end{array}_{\,S_2},
\begin{array}{|c|c|c|c|}\hline 1 & 2 & 4 & 5 \\ \hline 3 & \multicolumn{3}{c}{} \\ \cline{1-1}\end{array}_{\,S_3},
\begin{array}{|c|c|c|c|}\hline 1 & 3 & 4 & 5 \\ \hline 2 & \multicolumn{3}{c}{} \\ \cline{1-1}\end{array}_{\,S_4}. \tag{14}
$$

With the similar method, one obtains the spin wave functions for the $QQQQ\bar{q}$ pentaquark states with $J = 1/2$, which can be represented in partition [32] as

$$
\begin{array}{|c|c|c|}\hline 1 & 2 & 3 \\ \hline 4 & 5 & \multicolumn{1}{c}{} \\ \cline{1-2}\end{array}_{\,S_1},
\begin{array}{|c|c|c|}\hline 1 & 2 & 4 \\ \hline 3 & 5 & \multicolumn{1}{c}{} \\ \cline{1-2}\end{array}_{\,S_2},
\begin{array}{|c|c|c|}\hline 1 & 3 & 4 \\ \hline 2 & 5 & \multicolumn{1}{c}{} \\ \cline{1-2}\end{array}_{\,S_3},
\begin{array}{|c|c|c|}\hline 1 & 2 & 5 \\ \hline 3 & 4 & \multicolumn{1}{c}{} \\ \cline{1-2}\end{array}_{\,S_4},
\begin{array}{|c|c|c|}\hline 1 & 3 & 5 \\ \hline 2 & 4 & \multicolumn{1}{c}{} \\ \cline{1-2}\end{array}_{\,S_5}. \tag{15}
$$

Since particle 5 corresponds to a light antiquark, we can isolate this antiquark and discuss the symmetry property of the first four heavy quarks 1, 2, 3, and 4 in $\psi_{\mathrm{color}} \otimes \psi_{\mathrm{spin}}$ space.

When the antiquark 5 is separated from the spin wave functions, the spin states represented in Young tableaux without the antiquark 5 can be directly obtained from Eqs. (13)–(15) as

$$
\begin{aligned}
J = \frac{5}{2}:&\ \begin{array}{|c|c|c|c|}\hline 1 & 2 & 3 & 4 \\ \hline\end{array}_{\,S_1}, \\
J = \frac{3}{2}:&\ \begin{array}{|c|c|c|c|}\hline 1 & 2 & 3 & 4 \\ \hline\end{array}_{\,S_1},
\begin{array}{|c|c|c|}\hline 1 & 2 & 3 \\ \hline 4 & \multicolumn{2}{c}{} \\ \cline{1-1}\end{array}_{\,S_2},
\begin{array}{|c|c|c|}\hline 1 & 2 & 4 \\ \hline 3 & \multicolumn{2}{c}{} \\ \cline{1-1}\end{array}_{\,S_3},
\begin{array}{|c|c|c|}\hline 1 & 3 & 4 \\ \hline 2 & \multicolumn{2}{c}{} \\ \cline{1-1}\end{array}_{\,S_4}, \\
J = \frac{1}{2}:&\ \begin{array}{|c|c|c|}\hline 1 & 2 & 3 \\ \hline 4 & \multicolumn{2}{c}{} \\ \cline{1-1}\end{array}_{\,S_1},
\begin{array}{|c|c|c|}\hline 1 & 2 & 4 \\ \hline 3 & \multicolumn{2}{c}{} \\ \cline{1-1}\end{array}_{\,S_2},
\begin{array}{|c|c|c|}\hline 1 & 3 & 4 \\ \hline 2 & \multicolumn{2}{c}{} \\ \cline{1-1}\end{array}_{\,S_3},
\begin{array}{|c|c|}\hline 1 & 2 \\ \hline 3 & 4 \\ \hline\end{array}_{\,S_4},
\begin{array}{|c|c|}\hline 1 & 3 \\ \hline 2 & 4 \\ \hline\end{array}_{\,S_5}
\end{aligned} \tag{16}
$$

In Eq. (16), the spin states can be identified with the Young-Yamanouchi basis vectors for partitions [4], [31], and [22].

For constructing the $\psi_{\mathrm{flavor}} \otimes \psi_{\mathrm{color}} \otimes \psi_{\mathrm{spin}}$ wave functions of $QQQQ\bar{q}$ pentaquark system, we should combine the partition [211] of the color singlets in Eq. (9) with partitions [4], [31], [22] of the spin states in Eq. (16) by the inner product of the permutation group. Thus, the $\psi_{\mathrm{color}} \otimes \psi_{\mathrm{spin}}$ wave functions with a certain symmetry can be constructed. We get the corresponding Young diagram representations of $\psi_{\mathrm{color}} \otimes \psi_{\mathrm{spin}}$ bases [64–66],

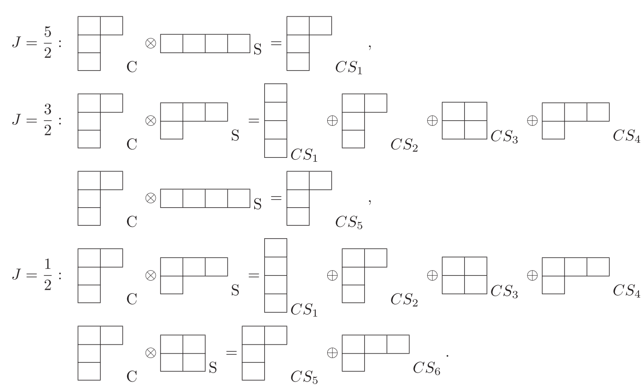

(17)

By using the Clebsch-Gordan (CG) coefficient of the permutation group S_n, one obtains the coupling scheme designed to construct the $\psi_{\mathrm{color}} \otimes \psi_{\mathrm{spin}}$ states. Here, any CG coefficient of S_n can be factorized into an isoscalar factor, called the K matrix, and the CG coefficient of S_{n-1} [65]. The expression of CG coefficient of S_n reads as

$$
\begin{aligned}
&S([f']p'q'y'[f'']p''q''y''|[f]pqy) \\
&= K([f']p'[f'']p''|[f]p)S([f'_{p'}]q'y'[f''_{p''}]q''y''|[f_p]qy).
\end{aligned} \tag{18}
$$

Here, S in the left-hand (right-hand) side denotes a CG coefficient of S_n (S_{n-1}) and $[f]$ ($[f_p]$) is a Young tableau of S_n (S_{n-1}) with $[f]pqy$ as a specific Young-Yamanouchi basis vector. And, p (q) is the row of the n ($n-1$)th particle in the Young-Yamanouchi basis vector, while y is the distribution of the $n-2$ remaining particles. In fact, a similar application is also used in Refs. [66–70]. According to the isoscalar factors for S_3 and S_4 in Tables 6.2 and 6.3 of Ref. [65], the corresponding CG coefficient of S_4 can be obtained. The corresponding Young-Yamanouchi basis vector obtained from the $\psi_{\rm color} \otimes \psi_{\rm spin}$ coupling [see Eq. (17)] is collected in Eq. (A1) of Appendix.

We can combine the flavor wave functions with the $\psi_{\rm color} \otimes \psi_{\rm spin}$ wave functions [see Eq. (A1)] of $QQQQ\bar{q}$ pentaquark states to deduce the symmetry allowed $\psi_{\rm flavor} \otimes \psi_{\rm color} \otimes \psi_{\rm spin}$ pentaquark wave functions. In Table VII in the Appendix, all the symmetrically allowed Young-Yamanouchi basis vectors for the different flavor wave functions are listed.

By constructing all the possible $\psi_{\rm flavor} \otimes \psi_{\rm color} \otimes \psi_{\rm spin}$ bases satisfied for $\{1234\}$, $\{123\}$, and $\{12\}\{34\}$ symmetry, we can calculate the CMI matrices for the studied pentaquark states. Here, we only present the expressions of CMI Hamiltonians for the $cccc\bar{n}$, $cccb\bar{n}$, and $ccbb\bar{n}$ pentaquark subsystems in Table VIII in the Appendix. According to their similar symmetry properties, the expressions of CMI matrices for other pentaquark subsystems can be deduced for those of the $cccc\bar{c}$, $cccb\bar{c}$, and $ccbb\bar{c}$ pentaquark subsystems.

III. MASS SPECTRA AND DECAY BEHAVIORS

As shown in Table III, according to symmetry properties, we can divide the $QQQQ\bar{q}$ pentaquark system into the following three groups:

(a) The $cccc\bar{q}$ and $bbbb\bar{q}$ pentaquark subsystems.
(b) The $cccb\bar{q}$ and $bbbc\bar{q}$ pentaquark subsystems.
(c) The $ccbb\bar{q}$ pentaquark subsystem.

For the $cccc\bar{q}$ and $bbbb\bar{q}$ subsystems, the wave functions should be antisymmetric for the exchange between the 12, 13, 14, 23, 24, or 34 particles. The $cccb\bar{q}$ and $bbbc\bar{q}$ wave functions are antisymmetric when exchanging the 12, 13, or 23 particles. However, for the $ccbb\bar{q}$ subsystem, the antisymmetry is considered only for exchanging the 12 or 34 particles. The fewer restrictions lead to more allowed wave functions. Therefore, the number of basis states in Table VII increases from $cccc\bar{n}$ to $cccb\bar{n}$ and next to $ccbb\bar{n}$ due to the Pauli principle. In the following, we will discuss the mass spectra and strong decay properties of $QQQQ\bar{q}$ pentaquark system group by group. All of them are explicitly exotic states. If such pentaquark states could be observed in an experiment, its pentaquark state nature could be easily identified. For simplicity, we use $\mathrm{P}_{\rm content}(\mathrm{mass}, I, J^P)$ to label a particular pentaquark state.

A. The $cccc\bar{q}$ and $bbbb\bar{q}$ pentaquark states

Here, we first discuss the $cccc\bar{q}$ and $bbbb\bar{q}$ pentaquark subsystems. Because of the symmetrical constraint from Pauli principle, i.e., fully antisymmetric among the first four charm quarks, the ground $J^P = 5/2^-$ pentaquark state with $cccc\bar{q}$ and $bbbb\bar{q}$ cannot exist. We only find two ground states: a $J^P = 3/2^-$ state and a $J^P = 1/2^-$ state for these subsystems.

Diagonalizing the Hamiltonians in Table VIII with the corresponding parameters in Table II, we can obtain the corresponding mass spectra for $cccc\bar{q}$ and $bbbb\bar{q}$ pentaquark subsystems and present them in Table IV. For the reference mass scheme, the only combination of meson-baryon reference systems are $(\Omega_{ccc}) + (D)$, $(\Omega_{ccc}) + (D_s)$, $(\Omega_{bbb}) + (\bar{B})$, and $(\Omega_{bbb}) + (\bar{B}_s)$ for the $cccc\bar{n}$, $cccc\bar{s}$, $bbbb\bar{n}$, and $bbbb\bar{s}$ subsystems, respectively.

The modified CMI model scheme takes the chromoelectric interaction explicitly compared to the reference mass scheme, and therefore we use the results in this scheme for the following analysis. Based on the results calculated from the modified CMI model scheme, we plot the mass spectra of the $cccc\bar{n}$, $cccc\bar{s}$, $bbbb\bar{n}$, and $bbbb\bar{s}$ subsystems in Figs. 2(a)–2(d), respectively. Moreover, we also plot all the baryon-meson thresholds which can decay to through quark rearrangement in Figs. 2(a)–2(d). Meanwhile, we label the spin of the baryon-meson states with superscript. When the spin of an initial pentaquark state is equal to the number in the superscript of a baryon-meson state, it may decay into that baryon-meson channel through an S wave. Here, we define the relatively "stable" pentaquark states as those which cannot decay into the S wave baryon-meson states. Meanwhile, we label these stable pentaquark states with $\diamond$ in the relevant figure and tables.

Based on the obtained $cccc\bar{q}$ and $bbbb\bar{q}$ pentaquark spectra, we can discuss the possible decay patterns by considering different rearrangement of quarks in the corresponding pentaquark states. The discussion of possible decay patterns for these pentaquark states would be helpful for the observation in experiments. From Figs. 2(a)–2(d), we can easily find that the $J^P = 3/2^-$ state generally has smaller masses than that of the $J^P = 1/2^-$ state in the $cccc\bar{q}$ and $bbbb\bar{q}$ pentaquark subsystems. We also find that all the $cccc\bar{q}$ and $bbbb\bar{q}$ pentaquark states have strong decay channels, which indicates that in the modified CMI model, no stable $cccc\bar{q}$ and $bbbb\bar{q}$ pentaquark exists.

In addition to the mass spectra, the eigenvectors of pentaquark states will also provide important information about the two-body strong decay of multiquark states [60–62,71–73]. The overlap for the pentaquark with a specific baryon $\otimes$ meson state can be calculated by transforming the eigenvectors of the pentaquark states into the baryon $\otimes$ meson configuration. In the $QQQ \otimes Q\bar{q}$ configuration, the color wave function of the pentaquark falls into two categories: the color-singlet $|(QQQ)^{1_c}(Q\bar{q})^{1_c}\rangle$ and

TABLE IV. The estimated masses for the $QQQQ\bar{q}$ ($Q = c, b; q = n, s; n = u, d$) system in units of MeV. The eigenvalues of H_{CMI} matrix are listed in the second column. The corresponding masses in the reference mass scheme are listed in the third and/or fourth column. The masses with the modified CMI model scheme are presented in the last column.

		Reference mass scheme		Modified CMI model scheme			Reference mass scheme		Modified CMI model scheme
		$cccc\bar{n}$					$cccc\bar{s}$		
J^P	Eigenvalue	$(D\Omega_{ccc})$		Mass	J^P	Eigenvalue	$(D_s\Omega_{ccc})$		Mass
$\frac{3}{2}^-$	26.4	6761		6761	$\frac{3}{2}^-$	25.9	6861		6864
$\frac{1}{2}^-$	132.0	6867		6867	$\frac{1}{2}^-$	133.1	6968		6972
		$bbbb\bar{n}$					$bbbb\bar{s}$		
J^P	Eigenvalue	$(B\Omega_{bbb})$		Mass	J^P	Eigenvalue	$(B_s\Omega_{bbb})$		Mass
$\frac{3}{2}^-$	22.4	19631		19647	$\frac{3}{2}^-$	21.3	19720		19736
$\frac{1}{2}^-$	56.0	19664		19681	$\frac{1}{2}^-$	58.1	19757		19773
		$cccb\bar{n}$					$cccb\bar{s}$		
J^P	Eigenvalue	$(B\Omega_{ccc})$	$(D\Omega_{ccb})$	Mass	J^P	Eigenvalue	$(B_s\Omega_{ccc})$	$(D_s\Omega_{ccb})$	Mass
$\frac{5}{2}^-$	37.6	10110	9816	10110	$\frac{5}{2}^-$	38.7	10202	9917	10201
$\frac{3}{2}^-$	65.3	10138	9843	10118	$\frac{3}{2}^-$	65.9	10229	9944	10210
	22.0	10094	9800	10078		21.3	10184	9900	10168
	−40.6	10032	9738	9961		−43.1	10120	9835	10062
$\frac{1}{2}^-$	110.4	10183	9889	10134	$\frac{1}{2}^-$	111.6	10275	9990	10228
	68.0	10140	9846	10062		69.1	10232	9948	10166
	−41.3	10031	9737	9946		−41.7	10121	9837	10047
		$bbbc\bar{n}$					$bbbc\bar{s}$		
J^P	Eigenvalue	$(D\Omega_{bbb})$	$(B\Omega_{bbc})$	Mass	J^P	Eigenvalue	$(D_s\Omega_{bbb})$	$(B_s\Omega_{bbc})$	Mass
$\frac{5}{2}^-$	49.6	16320	16544	16318	$\frac{5}{2}^-$	50.1	16421	16635	16422
$\frac{3}{2}^-$	49.6	16320	16544	16538	$\frac{3}{2}^-$	50.2	16421	16636	16626
	16.6	16287	16511	16318		16.1	16387	16601	16422
	−94.5	16176	16400	16176		−94.4	16274	16489	16277
$\frac{1}{2}^-$	72.2	16343	16567	16574	$\frac{1}{2}^-$	74.0	16445	16659	16663
	30.3	16301	16525	16523		31.8	16403	16617	16611
	−7.5	16263	16487	16315		−8.7	16362	16577	16418
		$ccbb\bar{n}$					$ccbb\bar{s}$		
J^P	Eigenvalue	$(B\Omega_{ccb})$	$(D\Omega_{bbc})$	Mass	J^P	Eigenvalue	$(B_s\Omega_{ccb})$	$(D_s\Omega_{bbc})$	Mass
$\frac{5}{2}^-$	42.1	13358	13199	13244	$\frac{5}{2}^-$	42.9	13450	13300	13341
$\frac{3}{2}^-$	61.2	13377	13218	13383	$\frac{3}{2}^-$	61.7	13468	13319	13470
	24.3	13340	13181	13231		24.1	13431	13281	13329
	11.3	13327	13168	13221		12.0	13419	13269	13319
	−70.4	13246	13086	13100		−72.6	13334	13185	13200
$\frac{1}{2}^-$	90.3	13406	13247	13414	$\frac{1}{2}^-$	91.7	13498	13349	13502
	44.8	13361	13202	13242		46.3	13453	13303	13343
	−5.4	13311	13151	13212		−7.3	13399	13250	13307
	−84.4	13232	13072	13086		−85.6	13321	13172	13187

the color-octet $|(QQQ)^{8_c}(Q\bar{q})^{8_c}\rangle$. The former one can easily dissociate into an S-wave baryon and meson [the so-called Okubo-Zweig-Iizuka (OZI)-superallowed decays], while the latter one cannot fall apart without the gluon exchange force. In this work, we only focus on the OZI-superallowed pentaquark decay process. It means that only the C_3 color part in Eq. (12) is considered in the color space.

For the two body decay via L-wave process, the expression describing partial decay width can be parametrized as [60,61]

$$\Gamma_i = \gamma_i \alpha \frac{k^{2L+1}}{m^{2L}} \cdot |c_i|^2, \tag{19}$$

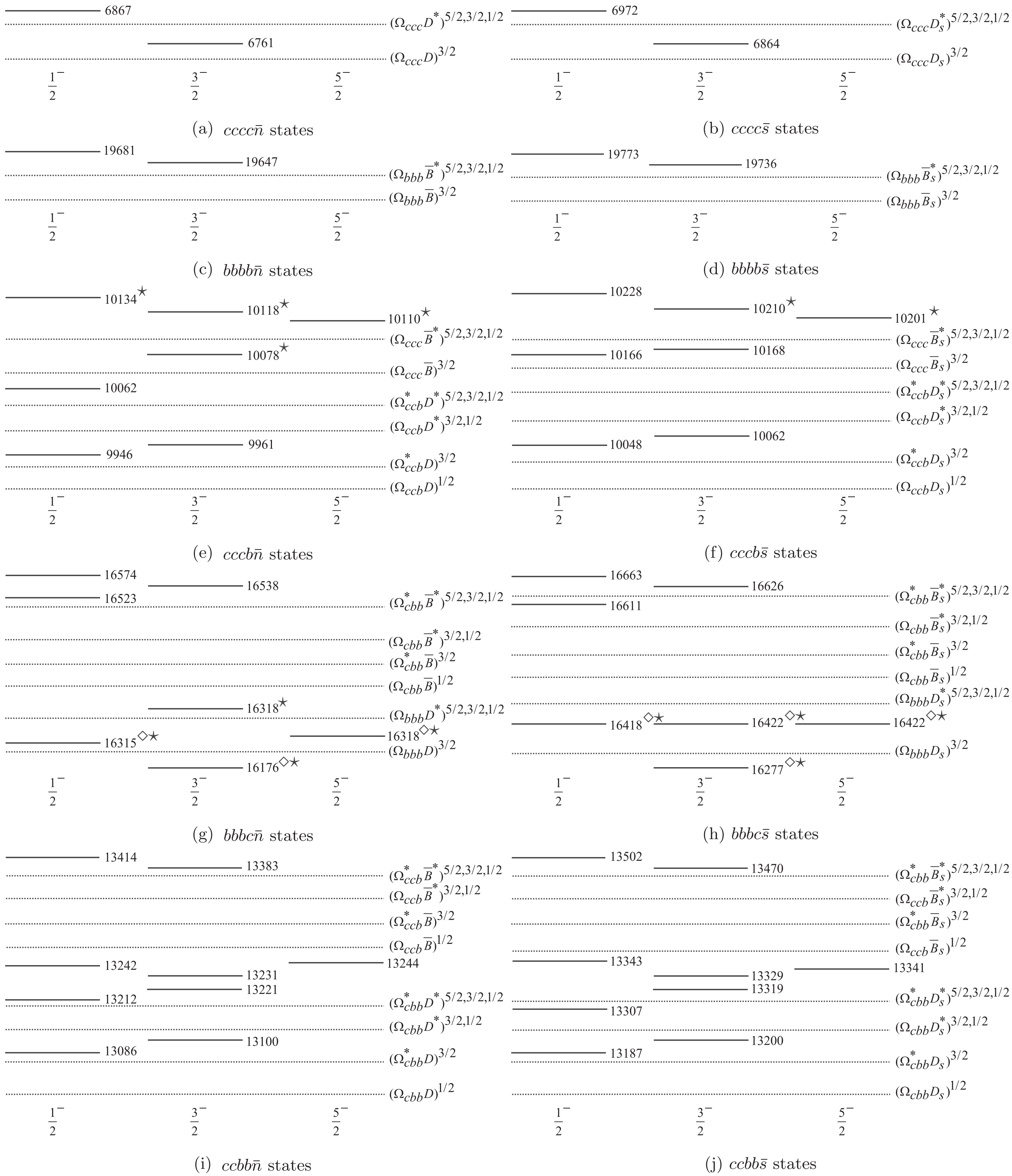

FIG. 2. Relative positions (unit: MeV) for the $cccc\bar{n}$, $cccc\bar{s}$, $bbbb\bar{n}$, $bbbb\bar{s}$, $cccb\bar{n}$, $cccb\bar{s}$, $bbbc\bar{n}$, $bbbc\bar{s}$, $ccbb\bar{n}$, and $ccbb\bar{s}$ pentaquark states labeled with solid lines. The dotted lines denote various S-wave baryon-meson thresholds, and the superscripts of the labels, e.g., $(\Omega_{ccc}D^*)^{5/2,3/2,1/2}$, represent the possible total angular momenta of the channels. We mark the relatively stable pentaquarks, unable to decay into the S-wave baryon-meson states, with "◇" after their masses. We mark the pentaquark whose wave function overlaps with that of one special baryon-meson state more than 90% with "⋆" after their masses.

where α is an effective coupling constant, m is the mass of the initial state, k is the momentum of the final states in the rest frame, and c_i is the overlap between the pentaquark wave function and the meson + baryon wave function. Take $P_{c^4\bar{n}}(6761, 1/2, 3/2^-) \to \Omega_{ccc}D^*$ as an example,

$$c_i \equiv \left\langle \Omega_{ccc} \otimes D^* \middle| P_{c^4\bar{n}}\left(6761, \frac{1}{2}, \frac{3^-}{2}\right) \right\rangle \tag{20}$$

$$= \left\langle (ccc)^{1_c}_{S=1/2} \otimes (c\bar{n})^{1_c}_{S=1} \middle| P_{c^4\bar{n}}\left(6761, \frac{1}{2}, \frac{3^-}{2}\right) \right\rangle = 0.456. \tag{21}$$

We show all possible overlaps between a pentaquark state and its possible $|(QQQ)^{1_c}(Q\bar{q})^{1_c}\rangle$ and $|(QQQ)^{1_c}(Q\bar{q})^{1_c}\rangle$ components in Table V. For the decay processes that we are interested in, $(\mathrm{k/m})^2$ is of $\mathcal{O}(10^{-2})$ or even smaller. Thus, we only consider the S-wave decays.

As for the γ_i, it depends on the spatial wave functions of initial and final states, and may not be the same for different decay processes. In the quark model, the spatial wave functions of the ground state scalar and vector meson are the same [61]. As a rough estimation, we introduce the following approximations to calculate the relative partial decay widths of the $cccc\bar{q}$ and $bbbb\bar{q}$ pentaquark states:

$$\gamma_{\Omega_{ccc}D^*} = \gamma_{\Omega_{ccc}D}, \qquad \gamma_{\Omega_{ccc}D_s^*} = \gamma_{\Omega_{ccc}D_s},$$
$$\gamma_{\Omega_{bbb}B^*} = \gamma_{\Omega_{bbb}B}, \qquad \gamma_{\Omega_{bbb}B_s^*} = \gamma_{\Omega_{bbb}B_s}. \tag{22}$$

We present $k \cdot |c_i|^2$ for each decay process in Table VI. From Table VI, one can roughly estimate the relative decay widths between different decay processes of different initial pentaquark states if neglecting the γ_i differences. Such approximation have already been applied in Refs. [55,56]. We emphasized that we are only interested in its relative partial decay widths between different decay modes for a particular pentaquark state.

Based on Eqs. (19)–(22), we can calculate relative partial decay widths for the $cccc\bar{q}$ and $bbbb\bar{q}$ pentaquark subsystems. For the $J^P = 1/2^-$ $cccc\bar{n}$ pentaquark state, it cannot decay into S-wave $\Omega_{ccc}D$ because of the constraint of angular conservation law. This same situation also happens in the $cccc\bar{s}$, $bbbb\bar{n}$, and $bbbb\bar{s}$ subsystems.

Due to small phase spaces, the $\mathrm{P}_{c^4\bar{n}}(6761, 1/2, 3/2^-)$ and $\mathrm{P}_{c^4\bar{s}}(6864, 0, 3/2^-)$ can only decay into $\Omega_{ccc}D$ and $\Omega_{ccc}D_s$ final states, respectively. While for the two $J^P = 3/2^-$ $bbbb\bar{q}$ pentaquark states, the $\mathrm{P}_{b^4\bar{n}}(19647, 1/2, 3/2^-)$ and $\mathrm{P}_{b^4\bar{s}}(19736, 0, 3/2^-)$, we find

$$\frac{\Gamma[P_{(b^4\bar{n})}(19647, 1/2, 3/2^-) \to \Omega_{bbb}B]}{\Gamma[P_{(b^4\bar{n})}(19647, 1/2, 3/2^-) \to \Omega_{bbb}B^*]} = 1.3 \tag{23}$$

and

$$\frac{\Gamma[P_{(b^4\bar{s})}(19736, 0, 3/2^-) \to \Omega_{bbb}B_s]}{\Gamma[P_{(b^4\bar{s})}(19736, 0, 3/2^-) \to \Omega_{bbb}B_s^*]} = 1.4, \tag{24}$$

respectively. Thus, the widths of the two modes do no differ very much.

B. The $cccb\bar{q}$ and $bbbc\bar{q}$ pentaquark states

Next, we consider the $cccb\bar{q}$ and $bbbc\bar{q}$ pentaquark subsystems. The $cccb\bar{q}$ and $bbbc\bar{q}$ pentaquark subsystems include three identical heavy quarks.

The masses of $cccb\bar{q}$ and $bbbc\bar{q}$ pentaquark states can be determined in two schemes and shown in Table IV. In the reference mass scheme, we can exhaust two types of baryon-meson reference systems. Specifically, we can use the $\Omega_{ccc} + B$ (B_s) and $\Omega_{ccb} + D$ (D_s) as reference systems to estimate the masses of the $cccb\bar{n}$ $(cccb\bar{s})$ pentaquark subsystem. Similarly, the meson-baryon reference systems $\Omega_{bbb} + D$ (D_s) and $\Omega_{bbc} + B$ (B_s) are used to calculate the masses of the $bbbc\bar{n}$ $(bbbc\bar{s})$ pentaquark subsystem. The obtained eigenvalues and masses of $cccb\bar{n}$ $(\bar{s})$ and $bbbc\bar{n}$ $(\bar{s})$ pentaquark states calculated from two types of reference systems are presented in the third and fourth columns of Table IV, respectively. We easily find that the mass spectra that come from two different reference systems differs by more than 100 MeV for some studied subsystems. The reason is that the dynamics and contributions from other terms in conventional meson and baryon potential are not elaborately considered in this model [50]. However, the mass gaps under different reference systems are still the same. Thus, if one pentaquark state were observed, its partner states may be searched for with the relative positions presented in Table IV.

Based on the results listed in the last column of Table IV, we plot the mass spectra and relevant quark rearrangement decay patterns for the $cccb\bar{n}$, $cccb\bar{s}$, $bbbc\bar{n}$, and $bbbc\bar{s}$ subsystems in Figs. 2(e)–2(h), respectively. Moreover, according to the modified CMI model, we can obtain the overlaps for $cccb\bar{n}$ $(cccb\bar{s})$ and $bbbc\bar{n}$ $(bbbc\bar{s})$ pentaquark states with different baryon $\otimes$ meson bases, and the results are shown in Table V.

From Table V, the $\mathrm{P}_{c^3b\bar{n}}(10110, 1/2, 5/2^-)$ state couples completely to the $\Omega_{ccc}\bar{B}^*$ system, which can be written as a direct product of a baryon Ω_{ccc} and a meson $\bar{B}^*$. Moreover, for the $\mathrm{P}_{c^3b\bar{n}}(10118, 1/2, 3/2^-)$, $\mathrm{P}_{c^3b\bar{n}}(10078, 1/2, 3/2^-)$, and $\mathrm{P}_{c^3b\bar{n}}(10134, 1/2, 1/2^-)$ states, they strongly couple to the $\Omega_{ccc}\bar{B}^*$, $\Omega_{ccc}\bar{B}$, and $\Omega_{ccc}\bar{B}^*$ bases, respectively. This kind of pentaquark behaves similar to the ordinary scattering state made of a baryon and meson if the inner interaction is not strong, but could also be a resonance or bound state dynamically generated by the baryon and meson with strong interaction. These kinds of pentaquarks deserve a more careful study with some hadron-hadron interaction models in future. Thus, we label them with ⋆ in Tables V, VI, and Fig. 2. Moreover, we find that the

TABLE V. The eigenvectors of the $ccc c\bar{n}$, $cccc\bar{s}$, $bbbb\bar{n}$, $bbbb\bar{s}$, $cccb\bar{n}$, $cccb\bar{s}$, $bbbc\bar{n}$, $bbbc\bar{s}$, $ccbb\bar{n}$, and $ccbb\bar{s}$ pentaquark subsystems. The masses are all in units of MeV. See the caption of Fig. 2 for meanings of ⋄ and ⋆.

		$ccc\otimes c\bar{n}$			$ccc\otimes c\bar{s}$			$bbb\otimes b\bar{n}$			$bbb\otimes b\bar{s}$	
J^P	Mass	$\Omega_{ccc}D^*$	$\Omega_{ccc}D$	Mass	$\Omega_{ccc}D_s^*$	$\Omega_{ccc}D_s$	Mass	$\Omega_{bbb}B^*$	$\Omega_{bbb}B$	Mass	$\Omega_{bbb}B_s^*$	$\Omega_{bbb}B_s$
$\frac{3}{2}^-$	6761	0.456	−0.354	6864	0.456	−0.354	19647	0.456	−0.354	19736	0.456	−0.354
$\frac{1}{2}^-$	6867	−0.577		6972	0.577		19681	−0.577		19773	0.577	

		$ccc\otimes b\bar{n}$		$ccb\otimes c\bar{n}$					$ccc\otimes b\bar{s}$		$ccb\otimes c\bar{s}$			
J^P	Mass	$\Omega_{ccc}B^*$	$\Omega_{ccc}B$	$\Omega^*_{ccb}D^*$	$\Omega^*_{ccb}D$	$\Omega_{ccb}D^*$	$\Omega_{ccb}D$	Mass	$\Omega_{ccc}B_s^*$	$\Omega_{ccc}B_s$	$\Omega^*_{ccb}D_s^*$	$\Omega^*_{ccb}D_s$	$\Omega_{ccb}D_s^*$	$\Omega_{ccb}D_s$
$\frac{5}{2}^-$	10110⋆	1.000		0.333				10201⋆	1.000		0.333			
$\frac{3}{2}^-$	10118⋆	0.950	0.188	0.217	0.140	−0.255		10210⋆	0.939	0.197	0.234	0.127	−0.258	
	10078⋆	−0.261	0.917	0.333	−0.019	0.174		10168	−0.289	0.895	0.345	−0.043	0.169	
	9961	0.172	0.352	0.372	−0.450	−0.230		10062	0.184	0.399	0.350	−0.452	−0.231	
$\frac{1}{2}^-$	10134⋆	0.914		−0.333		−0.201	−0.121	10228	0.891		−0.365		−0.188	−0.106
	10062	−0.246		0.498		−0.415	−0.064	10166	−0.290		0.477		−0.430	−0.065
	9946	0.323		0.220		0.397	−0.451	10048	0.349		0.217		0.387	−0.455

		$bbb\otimes c\bar{n}$		$bbc\otimes b\bar{n}$					$bbb\otimes c\bar{s}$		$bbc\otimes b\bar{s}$			
J^P	Mass	$\Omega_{bbb}D^*$	$\Omega_{bbb}D$	$\Omega^*_{bbc}B^*$	$\Omega^*_{bbc}B$	$\Omega_{bbc}B^*$	$\Omega_{bbc}B$	Mass	$\Omega_{bbb}D_s^*$	$\Omega_{bbb}D_s$	$\Omega^*_{bbc}B_s^*$	$\Omega^*_{bbc}B_s$	$\Omega_{bbc}B_s^*$	$\Omega_{bbc}B_s$
$\frac{5}{2}^-$	16318⋆⋄	1.000		0.333				16422⋆⋄	1.000		0.333			
$\frac{3}{2}^-$	16538	−0.004	−0.052	0.508	−0.375	−0.213		16626	−0.009	−0.056	0.509	−0.373	−0.213	
	16318⋆	0.999	−0.001	0.053	0.217	−0.139		16422⋆⋄	0.999	−0.001	0.051	0.218	−0.140	
	16176⋆⋄	0.001	0.999	0.189	0.187	0.204		16277⋆⋄	0.001	0.998	0.187	0.188	0.204	
$\frac{1}{2}^-$	16574	−0.085		−0.634		0.135	0.146	16663	−0.092		−0.634		0.139	0.141
	16523	−0.074		0.045		0.580	−0.323	16611	−0.086		0.052		0.580	−0.321
	16315⋆⋄	0.994		0.054		0.127	−0.130	16418⋆⋄	0.992		0.049		0.121	0.315

		$bbc\otimes c\bar{n}$				$ccb\otimes b\bar{n}$			
J^P	Mass	$\Omega^*_{bbc}D^*$	$\Omega^*_{bbc}D$	$\Omega_{bbc}D^*$	$\Omega_{bbc}D$	$\Omega^*_{ccb}B^*$	$\Omega^*_{ccb}B$	$\Omega_{ccb}B^*$	$\Omega_{ccb}B$
$\frac{5}{2}^-$	13244	−0.577				−0.577			
$\frac{3}{2}^-$	13383	−0.018	−0.052	−0.013		0.566	−0.372	0.452	
	13231	0.621	0.033	−0.072		−0.077	−0.454	−0.251	
	13221	−0.155	−0.167	−0.586		−0.319	−0.040	0.410	
	13100	0.250	−0.620	0.310		0.209	0.265	−0.096	
$\frac{1}{2}^-$	13414	−0.099		0.053	0.024	−0.710		−0.222	−0.317
	13242	0.641		0.220	−0.107	−0.124		0.385	0.180
	13212	0.197		−0.535	0.052	−0.078		−0.271	0.510
	13086	0.310		0.155	0.634	0.173		−0.301	−0.155

		$bbc\otimes c\bar{s}$				$ccb\otimes b\bar{s}$			
J^P	Mass	$\Omega^*_{bbc}D_s^*$	$\Omega^*_{bbc}D_s$	$\Omega_{bbc}D_s^*$	$\Omega_{bbc}D_s$	$\Omega^*_{ccb}B_s^*$	$\Omega^*_{ccb}B_s$	$\Omega_{ccb}B_s^*$	$\Omega_{ccb}B_s$
$\frac{5}{2}^-$	13341	−0.577				−0.577			
$\frac{3}{2}^-$	13470	−0.025	−0.056	−0.013		0.569	−0.366	0.453	
	13329	0.647	0.041	0.051		−0.122	−0.448	−0.167	
	13319	−0.041	−0.142	−0.596		−0.292	0.052	0.448	
	13200	−0.226	0.626	−0.293		0.218	0.282	−0.104	
$\frac{1}{2}^-$	13502	−0.109		0.057	0.025	−0.713		−0.220	−0.308
	13343	0.648		0.232	−0.085	−0.108		0.380	0.172
	13307	0.201		−0.531	0.055	−0.069		−0.265	0.515
	13187	0.286		0.150	0.637	−0.177		0.313	0.164

$J^P = 5/2^-$ $QQQQ'\bar{q}$ pentaquark states all have only one component $\Omega_{QQQ}B^*_{(s)}$ $(D^*_{(s)})$. Therefore, the $J^P = 5/2^-$ ground states are regarded as the states made of two hadrons.

For $cccb\bar{q}$ pentaquark states, they have two types of decay modes: $ccc - b\bar{q}$ and $ccb - c\bar{q}$. Similarly, the $bbbc\bar{q}$ pentaquark states also have two types of decay modes: $bbb - c\bar{q}$ and $bbc - b\bar{q}$. In the heavy quark limit, Ω^*_{ccb}

TABLE VI. The values of $k \cdot |c_i|^2$ for the $cccc\bar{n}$, $cccc\bar{s}$, $bbbb\bar{n}$, $bbbb\bar{s}$, $cccb\bar{n}$, $cccb\bar{s}$, $bbbc\bar{n}$, $bbbc\bar{s}$, $ccbb\bar{n}$, and $ccbb\bar{s}$ pentaquark states. The masses are all in units of MeV. The decay channel is marked with "×" if kinetically forbidden. See the caption of Fig. 2 for meanings of ◇ and ⋆. One can roughly estimate the relative decay widths between different decay processes of different initial pentaquark states with this table if neglecting the γ_i differences.

	$ccc\otimes c\bar{n}$			$ccc\otimes c\bar{s}$			$bbb\otimes b\bar{n}$			$bbb\otimes b\bar{s}$		
J^P	Mass	$\Omega_{ccc}D^*$	$\Omega_{ccc}D$	Mass	$\Omega_{ccc}D_s^*$	$\Omega_{ccc}D_s$	Mass	$\Omega_{bbb}B^*$	$\Omega_{bbb}B$	Mass	$\Omega_{bbb}B_s^*$	$\Omega_{bbb}B_s$
$\frac{3}{2}^-$	6761	×	67	6864	×	70	19647	66	84	19736	62	86
$\frac{1}{2}^-$	6867	151		6972	156		19681	201		19773	204	

		$ccc\otimes b\bar{n}$		$ccb\otimes c\bar{n}$					$ccc\otimes b\bar{s}$		$ccb\otimes c\bar{s}$			
J^P	Mass	$\Omega_{ccc}B^*$	$\Omega_{ccc}B$	$\Omega_{ccb}^*D^*$	Ω_{ccb}^*D	$\Omega_{ccb}D^*$	$\Omega_{ccb}D$	Mass	$\Omega_{ccc}B_s^*$	$\Omega_{ccc}B_s$	$\Omega_{ccb}^*D_s^*$	$\Omega_{ccb}^*D_s$	$\Omega_{ccb}D_s^*$	$\Omega_{ccb}D_s$
$\frac{5}{2}^-$	10110⋆	×		56				10201⋆	13		53			
$\frac{3}{2}^-$	10118⋆	173	18	25	17	40		10210⋆	184	21	28	14	40	
	10078⋆	×	217	43	0.3	15		10168	×	223	40	1	13	
	9961	×	×	×	94	×		10062	×	×	×	98	×	
$\frac{1}{2}^-$	10134⋆	291		64		27	14	10228	296		75		23	11
	10062	×		76		77	3	10166	×		75		86	3
	9946	×		×		×	104	10048	×		×		×	111

		$bbb\otimes c\bar{n}$		$bbc\otimes b\bar{n}$					$bbb\otimes c\bar{s}$		$bbc\otimes b\bar{s}$			
J^P	Mass	$\Omega_{bbb}D^*$	$\Omega_{bbb}D$	$\Omega_{bbc}^*B^*$	Ω_{bbc}^*B	$\Omega_{bbc}B^*$	$\Omega_{bbc}B$	Mass	$\Omega_{bbb}D_s^*$	$\Omega_{bbb}D_s$	$\Omega_{bbc}^*B_s^*$	$\Omega_{bbc}^*B_s$	$\Omega_{bbc}B_s^*$	$\Omega_{bbc}B_s$
$\frac{5}{2}^-$	16318⋆◇	×		×				16422⋆◇	×		×			
$\frac{3}{2}^-$	16538	0.02	3	89	94	27		16626	0.1	4	82	94	26	
	16318⋆	×	0.001	×	×	×		16422⋆◇	×	×	×	×	×	
	16176⋆◇	×	×	×	×	×		16277⋆◇	×	×	×	×	×	
$\frac{1}{2}^-$	16574	7		248		14	21	16663	8		247		15	20
	16523	5		0.2		164	79	16611	6		×		160	78
	16315⋆◇	×		×		×	×	16418⋆◇	×		×		×	×

		$bbc\otimes c\bar{n}$				$ccb\otimes b\bar{n}$			
J^P	Mass	$\Omega_{bbc}^*D^*$	Ω_{bbc}^*D	$\Omega_{bbc}D^*$	$\Omega_{bbc}D$	$\Omega_{ccb}^*B^*$	Ω_{ccb}^*B	$\Omega_{ccb}B^*$	$\Omega_{ccb}B$
$\frac{5}{2}^-$	13244	119				×			
$\frac{3}{2}^-$	13383	0.3	3	0.2		154	100	135	
	13231	111	0.8	2		×	×	×	
	13221	5	20	135		×	×	×	
	13100	×	127	×		×	×	×	
$\frac{1}{2}^-$	13414	8		3	0.7	332		39	96
	13242	142		23	9	×		×	×
	13212	5		101	2	×		×	×
	13086	×		×	164	×		×	×

		$bbc\otimes c\bar{s}$				$ccb\otimes b\bar{s}$			
J^P	Mass	$\Omega_{bbc}^*D_s^*$	$\Omega_{bbc}^*D_s$	$\Omega_{bbc}D_s^*$	$\Omega_{bbc}D_s$	$\Omega_{ccb}^*B_s^*$	$\Omega_{ccb}^*B_s$	$\Omega_{ccb}B_s^*$	$\Omega_{ccb}B_s$
$\frac{5}{2}^-$	13341	113				×			
$\frac{3}{2}^-$	13470	8	3	0.7		332	39	96	
	13329	142	23	9		×	×	×	
	13319	5	101	2		×	×	×	
	13200	×	×	164		×	×	×	
$\frac{1}{2}^-$	13502	10		3	0.7	328		38	92
	13343	148		26	6	×		×	×
	13307	×		92	2	×		×	×
	13187	×		×	173	×		×	×

(Ω^*_{bbc}) and Ω_{ccb} (Ω_{bbc}) have the same spatial wave function. Thus, for a $cccb\bar{q}$ or $bbbc\bar{q}$ pentaquark state, we use the following approximations:

$$\begin{aligned}
&\gamma_{\Omega^*_{ccb}D^*} = \gamma_{\Omega^*_{ccb}D} = \gamma_{\Omega_{ccb}D^*} = \gamma_{\Omega_{ccb}D}, \qquad \gamma_{\Omega_{ccc}B^*} = \gamma_{\Omega_{ccc}B},\\
&\gamma_{\Omega^*_{ccb}D^*_s} = \gamma_{\Omega^*_{ccb}D_s} = \gamma_{\Omega_{ccb}D^*_s} = \gamma_{\Omega_{ccb}D_s}, \qquad \gamma_{\Omega_{ccc}B^*_s} = \gamma_{\Omega_{ccc}B_s},\\
&\gamma_{\Omega^*_{bbc}B^*} = \gamma_{\Omega^*_{bbc}B} = \gamma_{\Omega_{bbc}B^*} = \gamma_{\Omega_{bbc}B}, \qquad \gamma_{\Omega_{bbb}D^*} = \gamma_{\Omega_{bbb}D},\\
&\gamma_{\Omega^*_{bbc}B^*_s} = \gamma_{\Omega^*_{bbc}B_s} = \gamma_{\Omega_{bbc}B^*_s} = \gamma_{\Omega_{bbc}B_s}, \qquad \gamma_{\Omega_{bbb}D^*_s} = \gamma_{\Omega_{bbb}D_s}.
\end{aligned} \tag{25}$$

Based on Table V, we obtain $k \cdot |c_i|^2$ for each $cccb\bar{q}$ and $bbbc\bar{q}$ pentaquark state and present them in Table VI.

As an example, we only concentrate on the $cccb\bar{n}$ pentaquark subsystem. According to Table VI, we can see that the $P_{c^3b\bar{n}}(9961, 1/2, 3/2^-)$ and $P_{c^3b\bar{n}}(9946, 1/2, 1/2^-)$ states only decay into $\Omega^*_{ccb}D$ and $\Omega_{ccb}D$ final states, respectively. For the $P_{c^3b\bar{n}}(10062, 1/2, 1/2^-)$ state, we have its relative partial decay width ratios as

$$\Gamma_{\Omega^*_{ccb}D^*} : \Gamma_{\Omega_{ccb}D^*} : \Gamma_{\Omega_{ccb}D} = 24:24:1, \tag{26}$$

which suggests that the partial decay width of the $\Omega^*_{ccb}D^*$ channel is nearly equal to that of the $\Omega_{ccb}D^*$ channel. Note that if a state would be observed in the decay pattern $\Omega^*_{ccb}D^*$, $\Omega^*_{ccb}D$, $\Omega^*_{ccb}D^*$, and $\Omega_{ccb}D$, it is a good candidate of a $cccb\bar{n}$ pentaquark state.

C. The $ccbb\bar{q}$ pentaquark states

The last group of the $QQQQ\bar{q}$ system is the pentaquark states with the $ccbb\bar{q}$ configuration. The $ccbb\bar{q}$ pentaquark states have two pairs of identical heavy quarks, the cc pair and bb pair. When we construct the wave functions of $ccbb\bar{q}$ pentaquark states, the Pauli principle should be satisfied simultaneously for these two pairs of heavy quarks.

In the reference mass scheme, there are also two types of meson-baryon reference systems for the $ccbb\bar{n}$ ($ccbb\bar{s}$) pentaquark subsystem, i.e., the $\Omega_{ccb} + B$ and $\Omega_{cbb} + D$ ($\Omega_{ccb} + B_s$ and $\Omega_{cbb} + D_s$).

Based on the results obtained from the modified CMI model in Table IV, we plot the mass spectra and possible decay patterns via rearrangement of constituent quarks in $ccbb\bar{n}$ and $ccbb\bar{s}$ pentaquark states in Figs. 2(i) and 2(j). According to Figs. 2(i) and 2(j), we find that all $ccbb\bar{n}$ and $ccbb\bar{s}$ pentaquark states have strong decay channels. i.e., from the modified CMI model analysis, there is no stable pentaquark state in $ccbb\bar{n}$ and $ccbb\bar{s}$ pentaquark subsystems.

To calculate the strong decay widths of the $ccbb\bar{n}$ and $ccbb\bar{s}$ pentaquark subsystems, we can use the following approximations:

$$\begin{aligned}
&\gamma_{\Omega^*_{cbb}D^*} = \gamma_{\Omega^*_{cbb}D} = \gamma_{\Omega_{cbb}D^*} = \gamma_{\Omega_{cbb}D},\\
&\gamma_{\Omega^*_{ccb}B^*} = \gamma_{\Omega^*_{ccb}B} = \gamma_{\Omega_{ccb}B^*} = \gamma_{\Omega_{ccb}B},\\
&\gamma_{\Omega^*_{cbb}D^*_s} = \gamma_{\Omega^*_{cbb}D_s} = \gamma_{\Omega_{cbb}D^*_s} = \gamma_{\Omega_{cbb}D_s},\\
&\gamma_{\Omega^*_{ccb}B^*_s} = \gamma_{\Omega^*_{ccb}B_s} = \gamma_{\Omega_{ccb}B^*_s} = \gamma_{\Omega_{ccb}B_s}.
\end{aligned} \tag{27}$$

By introducing the above relations, $k \cdot |c_i|^2$ for $ccbb\bar{n}$ ($ccbb\bar{s}$) pentaquark states can be obtained and we present them in Table VI.

To discuss the strong decay behaviors of the $ccbb\bar{n}$ ($\bar{s}$) pentaquark states, we mainly focus on the relative partial decay widths of the $ccbb\bar{n}$ subsystem, and the $ccbb\bar{s}$ subsystem can be analyzed in a similar way.

From Table VI, $J^P = 5/2^-$, the lowest $J^P = 3/2^-$, and the lowest $J^P = 1/2^-$ states can only decay into $\Omega^*_{cbb}D^*$, $\Omega^*_{cbb}D$, and $\Omega_{cbb}D$, respectively. The most important decay channel for the $P_{c^2b^2\bar{n}}(13383, 1/2, 3/2^-)$ is $\Omega^*_{bbc}D$ channel in $bbc - c\bar{n}$ decay mode. The highest $J^P = 3/2^-$ state $P_{c^2b^2\bar{n}}(13414, 1/2, 1/2^-)$ has many different decay channels and this state is expected to be broad. For $P_{c^2b^2\bar{n}}(13383, 1/2, 3/2^-)$, we have

$$\gamma_{\Omega^*_{cbb}D^*} : \gamma_{\Omega^*_{cbb}D} : \gamma_{\Omega_{cbb}D^*} = 1.5:15:1 \tag{28}$$

and

$$\gamma_{\Omega^*_{ccb}B^*} : \gamma_{\Omega^*_{ccb}B} : \gamma_{\Omega_{ccb}B^*} = 1.5:1:1.4. \tag{29}$$

For $P_{c^2b^2\bar{n}}(13414, 1/2, 1/2^-)$, we have

$$\gamma_{\Omega^*_{cbb}D^*} : \gamma_{\Omega_{cbb}D^*} : \gamma_{\Omega_{cbb}D} = 12:3.7:1 \tag{30}$$

and

$$\gamma_{\Omega^*_{ccb}B^*} : \gamma_{\Omega_{ccb}B^*} : \gamma_{\Omega_{ccb}B} = 3.5:0.4:1. \tag{31}$$

Obviously, its dominant decay modes in $cbb - c\bar{n}$ and $ccb - b\bar{n}$ sectors are $\Omega^*_{cbb}D^*$ and $\Omega^*_{ccb}B^*$ channels, respectively. Other three $J^P = 3/2^-$ and three $J^P = 1/2^-$ states only have $cbb - c\bar{n}$ decay mode. The $ccb - b\bar{n}$ decay modes are strongly suppressed by the corresponding phase space.

D. Comparison of other pentaquark systems

In 2020, the LHCb Collaboration studied the invariant mass spectrum of J/ψ pairs, and they reported a narrow structure around 6.9 GeV [74]. Taking this as an opportunity, the heavy flavored pentaquarks with four heavy quarks ($QQQQ\bar{q}$) and fully heavy pentaquarks ($QQQQ\bar{Q}$) are systematically discussed in this work and Ref. [57] within the modify CMI model. Here we can compare the differences between these two pentaquark systems.

First, we discuss the mass differences among the ground states of $QQQQ\bar{n}$, $QQQQ\bar{s}$, $QQQQ\bar{c}$, and $QQQQ\bar{b}$ with the same J^P. From Tables V and IV of Ref. [57], the masses of $cccc\bar{n}$, $cccc\bar{s}$, $cccc\bar{c}$, and $cccc\bar{b}$ ground states with $J^P = 3/2^-$ are 6761, 6864, 7864, and 11130 MeV, respectively. Moreover, relative to the $J^P = 1/2^-$ states, their corresponding mass gaps are 106, 108, 85, and 47 MeV, respectively. Other subsystems also have similar situations. Thus, compared with the $QQQQ\bar{Q}$ system, the $QQQQ\bar{q}$ system has lighter masses and bigger mass gaps when a heavy antiquark is replaced by a light antiquark because $v_{ij} \propto 1/m_i m_j$.

Second, we study the relations between the pentaquark and their corresponding baryon-meson channels. The fully heavy pentaquarks $QQQQ\bar{Q}$ are more likely below all possible strong decay channels and thus more stable compared to the $QQQQ\bar{q}$ systems. We have found two relatively stable states $\mathrm{P}_{c^2b^2\bar{b}}(17416, 0, 3/2^-)$ and $\mathrm{P}_{c^2b^2\bar{b}}(17477, 0, 5/2^-)$, which are below all allowed rearrangement decay channels in $QQQQ\bar{Q}$ system. However, we do not find any stable state for the $QQQQ\bar{q}$ multiquark systems. When both $QQQQ\bar{Q}$ and $QQQQ\bar{q}$ ground states are above their corresponding baryon-meson channel, the $QQQQ\bar{Q}$ mass would be closer to the threshold. For example, the $cccc\bar{n}$, $cccc\bar{s}$, $cccc\bar{c}$, and $cccc\bar{b}$ states are above the corresponding minimum threshold (Ω_{ccc}+ pseudoscalar meson) 106, 110, 94.5, and 69.5 MeV, respectively.

Unlike fully pentaquark $QQQQ\bar{Q}$, all $QQQQ\bar{q}$ pentaquark states can never mix with a triquark baryon and thus are explicit exotic states. An accurate measurement in a future experiment and the comparison may help us understand the $Q\bar{Q}$ annihilation effects in the hadron spectrum.

IV. SUMMARY

The observation of the $P_c(4312)$, $P_c(4440)$, and $P_c(4457)$ states achieved by the LHCb Collaboration and the study of the possible stable $QQ\bar{q}\bar{q}$ tetraquark states give us strong confidence to study the mass spectra of the $QQQQ\bar{q}$ pentaquark system within the framework of CMI model. Similar to the fully heavy $QQ\bar{Q}\bar{Q}$ tetraquark system [74], the $QQQQ\bar{q}$ system consists of four heavy quarks that are dominantly bounded by the gluon exchange interaction and can hardly be considered as molecular states.

In this work, by including the flavor SU(3) breaking effect, we first construct the $\psi_{\mathrm{flavor}} \otimes \psi_{\mathrm{color}} \otimes \psi_{\mathrm{spin}}$ wave functions based on the SU(2) and SU(3) symmetry and Pauli principle. Then we extract the effective coupling constants from the conventional hadrons. After that, we systematically calculate the chromomagnetic interaction Hamiltonian for the discussed pentaquark states and obtain the corresponding mass spectra. As a modification to the CMI model, the effect of chromoelectric interaction is added in the modified CMI model. So, we mainly discussed the results of mass spectra for the $QQQQ\bar{q}$ pentaquark system obtained from the modified CMI model. The results from the reference mass scheme are presented for comparison. In addition to the eigenvalues, we also provide the eigenvectors to extract useful information about the decay properties for the studied pentaquark systems. Finally, we analyze the stability, possible quark rearrangement decay channels, and relative partial decay widths for all the $QQQQ\bar{q}$ pentaquark states.

Due to the constraint from Pauli principle, there is no ground $J^P = 5/2^-$ $cccc\bar{q}$ and $bbbb\bar{q}$ pentaquark states. From the obtained tables and figures for the $QQQQ\bar{q}$ pentaquark system, we find no stable candidate in the modified CMI model. However, due to the uncertainty of the modified CMI model, some of them may not truly be unstable states, and further dynamical calculations may help us to clarify their natures. Especially, for some unstable states which are a little higher than the meson-baryon thresholds of lowest strong decay channels, they can be considered as narrow pentaquark states and have opportunities to be found in a future experiment. Meanwhile, the whole mass spectra have a slight shift or down due to the mass deviation of constituent quarks. While the mass gaps between different pentaquark states are relatively stable, if one pentaquark state is observed in the experiment, we can use these mass gaps to predict their corresponding multiplets.

Among the studied $QQQQ\bar{q}$ pentaquark states, all of them are explicit exotic states. If such pentaquark states are observed, their exotic nature can be easily identified. However, up to now, none of $QQQQ\bar{q}$ pentaquark states have been found. More detailed dynamical investigations on these pentaquark systems are still needed. Producing a $QQQQ\bar{q}$ pentaquark state seems to be a difficult task in the experiment. Our systematical study may provide theorists and experimentalists with some preliminary understanding toward this pentaquark system. We hope that the present study may inspire experimentalists and theorists to pay attention to this kind of pentaquark system.

ACKNOWLEDGMENTS

This work was supported by the China National Funds for Distinguished Young Scientists under Grant No. 11825503, National Key Research and Development Program of China under Contract No. 2020YFA0406400, the 111 Project under Grant No. B20063, and the National Natural Science Foundation of China under Grant No. 12047501. This project was also supported by the National Natural Science Foundation of China under Grants No. 11705072 and No. 11965016, CAS Interdisciplinary Innovation Team.

APPENDIX: SOME EXPRESSIONS IN DETAIL

The possible color ⊗ spin Young-Yamanouchi basis vectors of the Young tableaux in Eq. (17) are presented in Eq. (A1). We list the possible wave function satisfied by Pauli principle in Table VII and some CMI Hamiltonians in Table VIII.

$$
\begin{aligned}
J=\frac{5}{2}:\quad & \ytableaushort{13,2,4}_{CS_1} = \ytableaushort{13,2,4}_{C_2} \otimes \ytableaushort{1234}_{S_1};\\
& \ytableaushort{14,2,3}_{CS_2} = \ytableaushort{14,2,3}_{C_3} \otimes \ytableaushort{1234}_{S_1};\\
J=\frac{3}{2}:\quad & \ytableaushort{1,2,3,4}_{CS_1} = \frac{1}{\sqrt{3}}\ytableaushort{12,3,4}_{C_1} \otimes \ytableaushort{134,2}_{S_5} - \frac{1}{\sqrt{3}}\ytableaushort{13,2,4}_{C_2} \otimes \ytableaushort{124,3}_{S_4} + \frac{1}{\sqrt{3}}\ytableaushort{14,2,3}_{C_3} \otimes \ytableaushort{123,4}_{S_3};\\
& \ytableaushort{14,2,3}_{CS_2} = -\frac{1}{\sqrt{6}}\ytableaushort{12,3,4}_{C_1} \otimes \ytableaushort{134,2}_{S_5} + \frac{1}{\sqrt{6}}\ytableaushort{13,2,4}_{C_2} \otimes \ytableaushort{124,3}_{S_4} + \sqrt{\frac{2}{3}}\ytableaushort{14,2,3}_{C_3} \otimes \ytableaushort{123,4}_{S_3};\\
& \ytableaushort{13,2,4}_{CS_3} = \frac{1}{\sqrt{3}}\ytableaushort{12,3,4}_{C_1} \otimes \ytableaushort{134,2}_{S_5} - \frac{1}{\sqrt{6}}\ytableaushort{13,2,4}_{C_2} \otimes \ytableaushort{123,4}_{S_3} + \frac{1}{\sqrt{3}}\ytableaushort{13,2,4}_{C_2} \otimes \ytableaushort{124,3}_{S_4} + \frac{1}{\sqrt{6}}\ytableaushort{14,2,3}_{C_3} \otimes \ytableaushort{124,3}_{S_4};\\
& \ytableaushort{13,24}_{CS_4} = -\frac{1}{\sqrt{6}}\ytableaushort{12,3,4}_{C_1} \otimes \ytableaushort{134,2}_{S_5} - \frac{1}{\sqrt{3}}\ytableaushort{13,2,4}_{C_2} \otimes \ytableaushort{123,4}_{S_3} - \frac{1}{\sqrt{6}}\ytableaushort{13,2,4}_{C_2} \otimes \ytableaushort{124,3}_{S_4} + \frac{1}{\sqrt{3}}\ytableaushort{14,2,3}_{C_3} \otimes \ytableaushort{124,3}_{S_4};\\
& \ytableaushort{14,2,3}_{CS_5} = \ytableaushort{14,2,3}_{C_3} \otimes \ytableaushort{1234}_{S_2};\\
& \ytableaushort{13,2,4}_{CS_6} = \ytableaushort{13,2,4}_{C_2} \otimes \ytableaushort{1234}_{S_2}.\\
J=\frac{1}{2}:\quad & \ytableaushort{1,2,3,4}_{CS_1} = \frac{1}{\sqrt{3}}\ytableaushort{12,3,4}_{C_1} \otimes \ytableaushort{134,2}_{S_8} - \frac{1}{\sqrt{3}}\ytableaushort{13,2,4}_{C_2} \otimes \ytableaushort{124,3}_{S_7} + \frac{1}{\sqrt{3}}\ytableaushort{14,2,3}_{C_3} \otimes \ytableaushort{123,4}_{S_6};\\
& \ytableaushort{14,2,3}_{CS_2} = -\frac{1}{\sqrt{6}}\ytableaushort{12,3,4}_{C_1} \otimes \ytableaushort{134,2}_{S_8} + \frac{1}{\sqrt{6}}\ytableaushort{13,2,4}_{C_2} \otimes \ytableaushort{124,3}_{S_7} + \sqrt{\frac{2}{3}}\ytableaushort{14,2,3}_{C_3} \otimes \ytableaushort{123,4}_{S_6};\\
& \ytableaushort{13,2,4}_{CS_3} = \frac{1}{\sqrt{3}}\ytableaushort{12,3,4}_{C_1} \otimes \ytableaushort{134,2}_{S_8} - \frac{1}{\sqrt{6}}\ytableaushort{13,2,4}_{C_2} \otimes \ytableaushort{123,4}_{S_6} + \frac{1}{\sqrt{3}}\ytableaushort{13,2,4}_{C_2} \otimes \ytableaushort{134,2}_{S_7} + \frac{1}{\sqrt{6}}\ytableaushort{14,2,3}_{C_3} \otimes \ytableaushort{134,2}_{S_7};\\
& \ytableaushort{13,24}_{CS_4} = -\frac{1}{\sqrt{6}}\ytableaushort{12,3,4}_{C_1} \otimes \ytableaushort{134,2}_{S_8} - \frac{1}{\sqrt{3}}\ytableaushort{13,2,4}_{C_2} \otimes \ytableaushort{123,4}_{S_6} - \frac{1}{\sqrt{6}}\ytableaushort{13,2,4}_{C_2} \otimes \ytableaushort{124,3}_{S_7} + \frac{1}{\sqrt{3}}\ytableaushort{14,2,3}_{C_3} \otimes \ytableaushort{124,3}_{S_7};\\
& \ytableaushort{14,2,3}_{CS_5} = \frac{1}{\sqrt{2}}\ytableaushort{12,3,4}_{C_1} \otimes \ytableaushort{13,24}_{S_{10}} - \frac{1}{\sqrt{2}}\ytableaushort{13,2,4}_{C_2} \otimes \ytableaushort{12,34}_{S_9};\\
& \ytableaushort{13,2,4}_{CS_6} = \frac{1}{2}\ytableaushort{12,3,4}_{C_1} \otimes \ytableaushort{13,24}_{S_{10}} + \frac{1}{2}\ytableaushort{13,2,4}_{C_2} \otimes \ytableaushort{12,34}_{S_9} - \frac{1}{\sqrt{2}}\ytableaushort{14,2,3}_{C_3} \otimes \ytableaushort{12,34}_{S_9};
\end{aligned}
\tag{A1}
$$

TABLE VII. All possible color $\otimes$ spin Young-Yamanouchi basis vectors satisfied with Pauli principle for a specific $QQQQ\bar{q}$ [$q = n, s$ ($n = u, d$) and $Q = c, b$] subsystem. J represents the spin of the pentaquark states.

Flavor waves	J	The color $\otimes$ spin Young-Yamanouchi basis vectors
$cccc\bar{q}$ $bbbb\bar{q}$	$J = 3/2$	$\begin{array}{\|c\|}\hline 1\\\hline 2\\\hline 3\\\hline 4\\\hline\end{array}\ CS_1$
	$J = 1/2$	$\begin{array}{\|c\|}\hline 1\\\hline 2\\\hline 3\\\hline 4\\\hline\end{array}\ CS_1$
$cccb\bar{q}$ $bbbc\bar{q}$	$J = 5/2$	$\begin{array}{\|c\|c\|}\hline 1&4\\\hline 2\\\cline{1-1} 3\\\cline{1-1}\end{array}\ CS_1$
	$J = 3/2$	$\begin{array}{\|c\|}\hline 1\\\hline 2\\\hline 3\\\hline 4\\\hline\end{array}\ CS_1,\ \begin{array}{\|c\|c\|}\hline 1&4\\\hline 2\\\cline{1-1} 3\\\cline{1-1}\end{array}\ CS_2,\ \begin{array}{\|c\|c\|}\hline 1&4\\\hline 2\\\cline{1-1} 3\\\cline{1-1}\end{array}\ CS_5$
	$J = 1/2$	$\begin{array}{\|c\|}\hline 1\\\hline 2\\\hline 3\\\hline 4\\\hline\end{array}\ CS_1,\ \begin{array}{\|c\|c\|}\hline 1&4\\\hline 2\\\cline{1-1} 3\\\cline{1-1}\end{array}\ CS_2,\ \begin{array}{\|c\|c\|}\hline 1&4\\\hline 2\\\cline{1-1} 3\\\cline{1-1}\end{array}\ CS_5$
$ccbb\bar{q}$	$J = 5/2$	$\begin{array}{\|c\|c\|}\hline 1&4\\\hline 2\\\cline{1-1} 3\\\cline{1-1}\end{array}\ CS_1$
	$J = 3/2$	$\begin{array}{\|c\|}\hline 1\\\hline 2\\\hline 3\\\hline 4\\\hline\end{array}\ CS_1,\ \sqrt{\frac{2}{3}}\begin{array}{\|c\|c\|}\hline 1&3\\\hline 2\\\cline{1-1} 4\\\cline{1-1}\end{array}\ CS_3,\ -\sqrt{\frac{1}{3}}\begin{array}{\|c\|c\|}\hline 1&4\\\hline 2\\\cline{1-1} 3\\\cline{1-1}\end{array}\ CS_2,\ \begin{array}{\|c\|c\|}\hline 1&3\\\hline 2&4\\\hline\end{array}\ CS_4,\ \sqrt{\frac{2}{3}}\begin{array}{\|c\|c\|}\hline 1&3\\\hline 2\\\cline{1-1} 4\\\cline{1-1}\end{array}\ CS_6,\ -\sqrt{\frac{1}{3}}\begin{array}{\|c\|c\|}\hline 1&4\\\hline 2\\\cline{1-1} 3\\\cline{1-1}\end{array}\ CS_5$
	$J = 1/2$	$\begin{array}{\|c\|}\hline 1\\\hline 2\\\hline 3\\\hline 4\\\hline\end{array}\ CS_1,\ \sqrt{\frac{2}{3}}\begin{array}{\|c\|c\|}\hline 1&3\\\hline 2\\\cline{1-1} 4\\\cline{1-1}\end{array}\ CS_3,\ -\sqrt{\frac{1}{3}}\begin{array}{\|c\|c\|}\hline 1&4\\\hline 2\\\cline{1-1} 3\\\cline{1-1}\end{array}\ CS_2,\ \begin{array}{\|c\|c\|}\hline 1&3\\\hline 2&4\\\hline\end{array}\ CS_4,\ \sqrt{\frac{2}{3}}\begin{array}{\|c\|c\|}\hline 1&3\\\hline 2\\\cline{1-1} 4\\\cline{1-1}\end{array}\ CS_6,\ -\sqrt{\frac{1}{3}}\begin{array}{\|c\|c\|}\hline 1&4\\\hline 2\\\cline{1-1} 3\\\cline{1-1}\end{array}\ CS_5$

TABLE VIII. The expressions of CMI Hamiltonians for $cccc\bar{n}$, $cccb\bar{n}$, and $ccbb\bar{n}$ pentaquark subsystems. J represents the spin of the pentaquark states.

J	The expressions of CMI Hamiltonian for $cccc\bar{n}$ subsystem
$J = 3/2$	$\frac{56}{3}C_{cc} - \frac{16}{3}C_{c\bar{n}}$
$J = 1/2$	$\frac{56}{3}C_{cc} + \frac{32}{3}C_{c\bar{n}}$
J	The expressions of CMI Hamiltonian for $cccb\bar{n}$ subsystem
$J = 5/2$	$8C_{cc} + \frac{16}{3}C_{b\bar{n}}$
$J = 3/2$	$\begin{pmatrix} \left(\begin{array}{c}\frac{28}{3}C_{cc} + \frac{28}{3}C_{cb}\\ -4C_{c\bar{n}} - \frac{4}{3}C_{b\bar{n}}\end{array}\right) & \frac{2\sqrt{2}}{3}\left(\begin{array}{c}-C_{cc} + C_{cb}\\ +C_{c\bar{b}} - C_{b\bar{n}}\end{array}\right) & -\frac{8\sqrt{5}}{3}(C_{c\bar{n}} - C_{b\bar{n}}) \\ \frac{2\sqrt{2}}{3}\left(\begin{array}{c}-C_{cc} + C_{cb}\\ +C_{c\bar{b}} - C_{b\bar{n}}\end{array}\right) & \left(\begin{array}{c}\frac{26}{3}C_{cc} - 6C_{cb}\\ +\frac{2}{3}C_{c\bar{b}} - 2C_{b\bar{n}}\end{array}\right) & \frac{4\sqrt{10}}{3}(C_{c\bar{n}} + 2C_{b\bar{n}}) \\ -\frac{8\sqrt{5}}{3}(C_{c\bar{n}} - C_{b\bar{n}}) & \frac{4\sqrt{10}}{3}(C_{c\bar{n}} + 2C_{b\bar{n}}) & 8(C_{cc} - C_{b\bar{n}}) \end{pmatrix}$
$J = 1/2$	$\begin{pmatrix} \left(\begin{array}{c}\frac{28}{3}C_{cc} + \frac{28}{3}C_{cb}\\ +8C_{c\bar{n}} + \frac{8}{3}C_{b\bar{n}}\end{array}\right) & \frac{2\sqrt{2}}{3}\left(\begin{array}{c}-C_{cc} + C_{cb}\\ -2C_{c\bar{n}} + 2C_{b\bar{n}}\end{array}\right) & \frac{2\sqrt{2}}{3}(C_{c\bar{n}} - C_{b\bar{n}}) \\ \frac{2\sqrt{2}}{3}\left(\begin{array}{c}-C_{cc} + C_{cb}\\ -2C_{c\bar{n}} + 2C_{b\bar{n}}\end{array}\right) & \left(\begin{array}{c}\frac{26}{3}C_{cc} - 6C_{cb}\\ -\frac{4}{3}C_{c\bar{n}} + 4C_{b\bar{n}}\end{array}\right) & -\frac{2}{3}(13C_{c\bar{n}} - C_{b\bar{n}}) \\ \frac{2\sqrt{2}}{3}(C_{c\bar{n}} - C_{b\bar{n}}) & -\frac{2}{3}(13C_{c\bar{n}} - C_{b\bar{n}}) & 10(C_{cc} - C_{cb}) \end{pmatrix}$
J	The expressions of CMI Hamiltonian for $ccbb\bar{n}$ subsystem
$J = 5/2$	$\frac{8}{3}(C_{cc} + C_{bb} + C_{cb} + C_{c\bar{b}} + C_{b\bar{n}})$

(Table continued)

TABLE VIII. *(Continued)*

J	The expressions of CMI Hamiltonian for $cccc\bar{n}$ subsystem
$J=3/2$	$\begin{pmatrix} \left(\begin{smallmatrix} \frac{28}{9}C_{cc}+\frac{28}{9}C_{bb}+\frac{112}{9}C_{cb} \\ -\frac{8}{3}C_{c\bar{n}}-\frac{8}{3}C_{b\bar{n}} \end{smallmatrix}\right) & \frac{2}{3}\sqrt{\frac{2}{3}}\left(\begin{smallmatrix} C_{cc}-C_{bb} \\ -2C_{c\bar{n}}+2C_{b\bar{n}} \end{smallmatrix}\right) & -\frac{2\sqrt{2}}{9}(C_{cc}+C_{bb}+2C_{cb}) & \frac{16}{3}\sqrt{\frac{5}{3}}(C_{c\bar{n}}-C_{b\bar{n}}) \\ \frac{2}{3}\sqrt{\frac{2}{3}}\left(\begin{smallmatrix} C_{cc}-C_{bb} \\ -2C_{c\bar{n}}+2C_{b\bar{n}} \end{smallmatrix}\right) & \left(\begin{smallmatrix} \frac{10}{3}C_{cc}+\frac{10}{3}C_{bb}-4C_{cb} \\ -\frac{2}{3}C_{c\bar{n}}-\frac{2}{3}C_{b\bar{n}} \end{smallmatrix}\right) & -\frac{2}{3\sqrt{3}}\left(\begin{smallmatrix} C_{nn}-C_{bb} \\ +7C_{c\bar{n}}-7C_{b\bar{n}} \end{smallmatrix}\right) & 2\sqrt{10}(C_{c\bar{n}}+C_{b\bar{n}}) \\ -\frac{2\sqrt{2}}{9}(C_{cc}+C_{bb}+2C_{cb}) & -\frac{2}{3\sqrt{3}}\left(\begin{smallmatrix} C_{nn}-C_{bb} \\ +7C_{c\bar{n}}-7C_{b\bar{n}} \end{smallmatrix}\right) & \left(\begin{smallmatrix} \frac{26}{9}C_{cc}+\frac{26}{9}C_{bb}-\frac{100}{9}C_{cb} \\ +\frac{10}{3}C_{c\bar{n}}+\frac{10}{3}C_{b\bar{n}} \end{smallmatrix}\right) & -\frac{2}{3}\sqrt{\frac{10}{3}}(C_{c\bar{n}}-C_{b\bar{n}}) \\ \frac{16}{3}\sqrt{\frac{5}{3}}(C_{c\bar{n}}-C_{b\bar{n}}) & 2\sqrt{10}(C_{c\bar{n}}+C_{b\bar{n}}) & -\frac{2}{3}\sqrt{\frac{10}{3}}(C_{c\bar{n}}-C_{b\bar{n}}) & \left(\begin{smallmatrix} \frac{8}{3}C_{cc}+\frac{8}{3}C_{bb}+\frac{8}{3} \\ C_{cb}-4C_{c\bar{n}}-4C_{b\bar{n}} \end{smallmatrix}\right) \end{pmatrix}$
$J=1/2$	$\begin{pmatrix} \left(\begin{smallmatrix} \frac{28}{9}C_{cc}+\frac{28}{9}C_{bb}+\frac{112}{9}C_{cb} \\ +\frac{16}{3}C_{c\bar{n}}+\frac{16}{3}C_{b\bar{n}} \end{smallmatrix}\right) & \frac{2}{3}\sqrt{\frac{2}{3}}\left(\begin{smallmatrix} C_{cc}-C_{bb} \\ +4C_{c\bar{n}}-4C_{b\bar{n}} \end{smallmatrix}\right) & -\frac{2\sqrt{2}}{9}(C_{cc}+C_{bb}+2C_{cb}) & -\frac{4}{3}\sqrt{\frac{2}{3}}(C_{c\bar{n}}-C_{b\bar{n}}) \\ \frac{2}{3}\sqrt{\frac{2}{3}}\left(\begin{smallmatrix} C_{cc}-C_{bb} \\ +4C_{c\bar{n}}-4C_{b\bar{n}} \end{smallmatrix}\right) & \left(\begin{smallmatrix} \frac{10}{3}C_{cc}+\frac{10}{3}C_{bb}-4C_{cb} \\ +\frac{4}{3}C_{c\bar{n}}+\frac{4}{3}C_{b\bar{n}} \end{smallmatrix}\right) & -\frac{2}{3\sqrt{3}}\left(\begin{smallmatrix} C_{cc}-C_{bb} \\ -14C_{c\bar{n}}+14C_{b\bar{n}} \end{smallmatrix}\right) & -4(C_{c\bar{n}}+C_{b\bar{n}}) \\ -\frac{2\sqrt{2}}{9}(C_{cc}+C_{bb}+2C_{cb}) & -\frac{2}{3\sqrt{3}}\left(\begin{smallmatrix} C_{cc}-C_{bb} \\ -14C_{c\bar{n}}+14C_{b\bar{n}} \end{smallmatrix}\right) & \left(\begin{smallmatrix} \frac{26}{9}C_{cc}+\frac{26}{9}C_{bb}-\frac{100}{9}C_{cb} \\ -\frac{20}{3}C_{c\bar{n}}-\frac{20}{3}C_{b\bar{n}} \end{smallmatrix}\right) & \frac{28}{3\sqrt{3}}(C_{c\bar{n}}-C_{b\bar{n}}) \\ -\frac{4}{3}\sqrt{\frac{2}{3}}(C_{c\bar{n}}-C_{b\bar{n}}) & -4(C_{c\bar{n}}+C_{b\bar{n}}) & \frac{28}{3\sqrt{3}}(C_{c\bar{n}}-C_{b\bar{n}}) & \frac{8}{3}(C_{cc}+C_{bb}-2C_{cb}) \end{pmatrix}$

[1] http://lhcb-public.web.cern.ch/.

[2] M. Gell-Mann, A schematic model of baryons and mesons, Phys. Lett. **8**, 214 (1964).

[3] G. Zweig, An SU(3) model for strong interaction symmetry and its breaking. Version 1, CERN-TH-401.

[4] G. Zweig, An SU(3) model for strong interaction symmetry and its breaking. Version 2, CERN-TH-412.

[5] R. Aaij *et al.* (LHCb Collaboration), Observation of $J/\psi p$ Resonances Consistent with Pentaquark States in $\Lambda_b^0 \to J/\psi K^- p$ Decays, Phys. Rev. Lett. **115**, 072001 (2015).

[6] R. Aaij *et al.* (LHCb Collaboration), Model-Independent Evidence for $J/\psi p$ Contributions to $\Lambda_b^0 \to J/\psi p K^-$ Decays, Phys. Rev. Lett. **117**, 082002 (2016).

[7] R. Aaij *et al.* (LHCb Collaboration), Observation of a Narrow Pentaquark State, $P_c(4312)^+$, and of Two-Peak Structure of the $P_c(4450)^+$, Phys. Rev. Lett. **122**, 222001 (2019).

[8] R. Chen, X. Liu, X. Q. Li, and S. L. Zhu, Identifying Exotic Hidden-Charm Pentaquarks, Phys. Rev. Lett. **115**, 132002 (2015).

[9] H. X. Chen, W. Chen, X. Liu, T. G. Steele, and S. L. Zhu, Towards Exotic Hidden-Charm Pentaquarks in QCD, Phys. Rev. Lett. **115**, 172001 (2015).

[10] J. He, $\bar{D}\Sigma_c^*$ and $\bar{D}^*\Sigma_c$ interactions and the LHCb hidden-charmed pentaquarks, Phys. Lett. B **753**, 547 (2016).

[11] R. Chen, Z. F. Sun, X. Liu, and S. L. Zhu, Strong LHCb evidence supporting the existence of the hidden-charm molecular pentaquarks, Phys. Rev. D **100**, 011502 (2019).

[12] B. Wang, L. Meng, and S. L. Zhu, Hidden-charm and hidden-bottom molecular pentaquarks in chiral effective field theory, J. High Energy Phys. 11 (2019) 108.

[13] J. He and D. Y. Chen, Molecular states from $\Sigma_c^{(*)}\bar{D}^{(*)} - \Lambda_c\bar{D}^{(*)}$ interaction, Eur. Phys. J. C **79**, 887 (2019).

[14] M. Z. Liu, T. W. Wu, M. Sánchez Sánchez, M. P. Valderrama, L. S. Geng, and J. J. Xie, Spin-parities of the $P_c(4440)$ and $P_c(4457)$ in the one-boson-exchange model, Phys. Rev. D **103**, 054004 (2021).

[15] T. J. Burns and E. S. Swanson, Molecular interpretation of the $P_c(4440)$ and $P_c(4457)$ states, Phys. Rev. D **100**, 114033 (2019).

[16] C. Gignoux, B. Silvestre-Brac, and J. M. Richard, Possibility of stable multi-quark baryons, Phys. Lett. B **193**, 323 (1987).

[17] H. J. Lipkin, New possibilities for exotic hadrons: Anticharmed strange baryons, Phys. Lett. B **195**, 484 (1987).

[18] J. Leandri and B. Silvestre-Brac, Systematics of $\bar{Q}Q^-4$ systems with a pure chromomagnetic interaction, Phys. Rev. D **40**, 2340 (1989).

[19] M. Genovese, J. M. Richard, F. Stancu, and S. Pepin, Heavy flavor pentaquarks in a chiral constituent quark model, Phys. Lett. B **425**, 171 (1998).

[20] H. Y. Gao and B. Q. Ma, Exotic hadrons of minimal pentaquark (q q q q anti-q) states, Mod. Phys. Lett. A **14**, 2313 (1999).

[21] S. M. Gerasyuta and V. I. Kochkin, Relativistic quark model and pentaquark spectroscopy, Int. J. Mod. Phys. E **12**, 793 (2003).

[22] H. J. Lipkin, Pentaquark update after ten years, Nucl. Phys. **A625**, 207 (1997).

[23] T. Nakano *et al.* (LEPS Collaboration), Evidence for a Narrow $S=+1$ Baryon Resonance in Photoproduction from the Neutron, Phys. Rev. Lett. **91**, 012002 (2003).

[24] J. L. Rosner, Exotic states of matter in heavy meson decays, Phys. Rev. D **69**, 094014 (2004).
[25] H. X. Chen, W. Chen, X. Liu, and S. L. Zhu, The hidden-charm pentaquark and tetraquark states, Phys. Rep. **639**, 1 (2016).
[26] M. Karliner, J. L. Rosner, and T. Skwarnicki, Multiquark states, Annu. Rev. Nucl. Part. Sci. **68**, 17 (2018).
[27] Y. R. Liu, H. X. Chen, W. Chen, X. Liu, and S. L. Zhu, Pentaquark and tetraquark states, Prog. Part. Nucl. Phys. **107**, 237 (2019).
[28] J. Z. Bai *et al.* (BES Collaboration), Search for the pentaquark state in $\psi(2S)$ and J/ψ decays to $K_s^0 pK^- \bar{n}$ and $K_s^0 pK^+ n$, Phys. Rev. D **70**, 012004 (2004).
[29] B. Aubert *et al.* (*BABAR* Collaboration), Search for Strange-Pentaquark Production in e^+e^- Annihilation at $\sqrt{s} = 10.58$ GeV, Phys. Rev. Lett. **95**, 042002 (2005).
[30] M. Z. Wang *et al.* (Belle Collaboration), Study of the baryon-antibaryon low-mass enhancements in charmless three-body baryonic B decays, Phys. Lett. B **617**, 141 (2005).
[31] D. O. Litvintsev (CDF Collaboration), Pentaquark searches at CDF, Nucl. Phys. B, Proc. Suppl. **142**, 374 (2005).
[32] F. K. Guo, C. Hanhart, Q. Wang, and Q. Zhao, Could the near-threshold XYZ states be simply kinematic effects?, Phys. Rev. D **91**, 051504 (2015).
[33] A. Esposito, A. L. Guerrieri, F. Piccinini, A. Pilloni, and A. D. Polosa, Four-quark hadrons: An updated review, Int. J. Mod. Phys. A **30**, 1530002 (2015).
[34] A. Ali, J. S. Lange, and S. Stone, Exotics: Heavy pentaquarks and tetraquarks, Prog. Part. Nucl. Phys. **97**, 123 (2017).
[35] N. Brambilla, S. Eidelman, C. Hanhart, A. Nefediev, C. P. Shen, C. E. Thomas, A. Vairo, and C. Z. Yuan, The XYZ states: Experimental and theoretical status and perspectives, Phys. Rep. **873**, 1 (2020).
[36] A. Hosaka, T. Iijima, K. Miyabayashi, Y. Sakai, and S. Yasui, Exotic hadrons with heavy flavors: X, Y, Z, and related states, Prog. Theor. Exp. Phys. **2016**, 062C01 (2016).
[37] J. M. Richard, Exotic hadrons: Review and perspectives, Few Body Syst. **57**, 1185 (2016).
[38] R. F. Lebed, R. E. Mitchell, and E. S. Swanson, Heavy-quark QCD exotica, Prog. Part. Nucl. Phys. **93**, 143 (2017).
[39] A. Esposito, A. Pilloni, and A. D. Polosa, Multiquark resonances, Phys. Rep. **668**, 1 (2017).
[40] R. Aaij *et al.* (LHCb Collaboration), Observation of the Doubly Charmed Baryon Ξ_{cc}^{++}, Phys. Rev. Lett. **119**, 112001 (2017).
[41] S. Q. Luo, K. Chen, X. Liu, Y. R. Liu, and S. L. Zhu, Exotic tetraquark states with the $qq\bar{Q}\bar{Q}$ configuration, Eur. Phys. J. C **77**, 709 (2017).
[42] M. Karliner and J. L. Rosner, Discovery of Doubly-Charmed Ξ_{cc} Baryon Implies a Stable ($bb\bar{u}\bar{d}$) Tetraquark, Phys. Rev. Lett. **119**, 202001 (2017).
[43] E. J. Eichten and C. Quigg, Heavy-Quark Symmetry Implies Stable Heavy Tetraquark Mesons $Q_iQ_j\bar{q}_k\bar{q}_l$, Phys. Rev. Lett. **119**, 202002 (2017).
[44] A. De Rujula, H. Georgi, and S. L. Glashow, Hadron masses in a gauge theory, Phys. Rev. D **12**, 147 (1975).
[45] K. Chen, X. Liu, J. Wu, Y. R. Liu, and S. L. Zhu, Triply heavy tetraquark states with the $QQ\bar{Q}\bar{q}$ configuration, Eur. Phys. J. A **53**, 5 (2017).
[46] J. Wu, Y. R. Liu, K. Chen, X. Liu, and S. L. Zhu, Heavy-flavored tetraquark states with the $QQ\bar{Q}\bar{Q}$ configuration, Phys. Rev. D **97**, 094015 (2018).
[47] J. Wu, Y. R. Liu, K. Chen, X. Liu, and S. L. Zhu, $X(4140)$, $X(4270)$, $X(4500)$ and $X(4700)$ and their $cs\bar{c}\bar{s}$ tetraquark partners, Phys. Rev. D **94**, 094031 (2016).
[48] J. Wu, X. Liu, Y. R. Liu, and S. L. Zhu, Systematic studies of charmonium-, bottomonium-, and B_c-like tetraquark states, Phys. Rev. D **99**, 014037 (2019).
[49] J. Wu, Y. R. Liu, K. Chen, X. Liu, and S. L. Zhu, Hidden-charm pentaquarks and their hidden-bottom and B_c-like partner states, Phys. Rev. D **95**, 034002 (2017).
[50] Q. S. Zhou, K. Chen, X. Liu, Y. R. Liu, and S. L. Zhu, Surveying exotic pentaquarks with the typical $QQqq\bar{q}$ configuration, Phys. Rev. C **98**, 045204 (2018).
[51] S. Y. Li, Y. R. Liu, Y. N. Liu, Z. G. Si, and J. Wu, Pentaquark states with the $QQQq\bar{q}$ configuration in a simple model, Eur. Phys. J. C **79**, 87 (2019).
[52] H. T. An, Q. S. Zhou, Z. W. Liu, Y. R. Liu, and X. Liu, Exotic pentaquark states with the $qqQQ\bar{Q}$ configuration, Phys. Rev. D **100**, 056004 (2019).
[53] Y. R. Liu, X. Liu, and S. L. Zhu, $X(5568)$ and and its partner states, Phys. Rev. D **93**, 074023 (2016).
[54] J. B. Cheng and Y. R. Liu, Understanding the structures of hidden-charm pentaquarks in a simple model, Nucl. Part. Phys. Proc. **309–311**, 158 (2020).
[55] J. B. Cheng and Y. R. Liu, $P_c(4457)^+$, $P_c(4440)^+$, and $P_c(4312)^+$: Molecules or compact pentaquarks?, Phys. Rev. D **100**, 054002 (2019).
[56] J. B. Cheng, S. Y. Li, Y. R. Liu, Y. N. Liu, Z. G. Si, and T. Yao, Spectrum and rearrangement decays of tetraquark states with four different flavors, Phys. Rev. D **101**, 114017 (2020).
[57] H. T. An, K. Chen, Z. W. Liu, and X. Liu, Fully heavy pentaquarks, Phys. Rev. D **103**, 074006 (2021).
[58] H. Hgaasen, E. Kou, J. M. Richard, and P. Sorba, Isovector and hidden-beauty partners of the X(3872), Phys. Lett. B **732**, 97 (2014).
[59] X. Z. Weng, X. L. Chen, and W. Z. Deng, Masses of doubly heavy-quark baryons in an extended chromomagnetic model, Phys. Rev. D **97**, 054008 (2018).
[60] X. Z. Weng, X. L. Chen, W. Z. Deng, and S. L. Zhu, Systematics of fully heavy tetraquarks, Phys. Rev. D **103**, 034001 (2021).
[61] X. Z. Weng, X. L. Chen, W. Z. Deng, and S. L. Zhu, Hidden-charm pentaquarks and P_c states, Phys. Rev. D **100**, 016014 (2019).
[62] L. Zhao, W. Z. Deng, and S. L. Zhu, Hidden-charm tetraquarks and charged Z_c states, Phys. Rev. D **90**, 094031 (2014).
[63] M. Tanabashi *et al.* (Particle Data Group), Review of particle physics, Phys. Rev. D **98**, 030001 (2018).
[64] C. Itzykson and M. Nauenberg, Unitary groups: Representation and decompositions, Rev. Mod. Phys. **38**, 95 (1966).
[65] F. Stancu and S. Pepin, Isoscalar factors of the permutation group, Few Body Syst. **26**, 113 (1999).

[66] W. Park, A. Park, S. Cho, and S. H. Lee, $P_c(4380)$ in a constituent quark model, Phys. Rev. D **95**, 054027 (2017).
[67] W. Park, A. Park, and S. H. Lee, Dibaryons in a constituent quark model, Phys. Rev. D **92**, 014037 (2015).
[68] A. Park, W. Park, and S. H. Lee, Dibaryons with two strange quarks and one heavy flavor in a constituent quark model, Phys. Rev. D **94**, 054027 (2016).
[69] W. Park, A. Park, and S. H. Lee, Dibaryons with two strange quarks and total spin zero in a constituent quark model, Phys. Rev. D **93**, 074007 (2016).
[70] W. Park, S. Cho, and S. H. Lee, Where is the stable pentaquark?, Phys. Rev. D **99**, 094023 (2019).
[71] R. L. Jaffe, Multi-quark hadrons. 1. The phenomenology of (2 quark 2 anti-quark) mesons, Phys. Rev. D **15**, 267 (1977).
[72] D. Strottman, Multi-quark baryons and the MIT bag model, Phys. Rev. D **20**, 748 (1979).
[73] Z. G. Wang, Analysis of $P_c(4380)$ and $P_c(4450)$ as pentaquark states in the diquark model with QCD sum rules, Eur. Phys. J. C **76**, 70 (2016).
[74] R. Aaij *et al.* (LHCb Collaboration), Observation of structure in the J/ψ -pair mass spectrum, Sci. Bull. **65**, 1983 (2020).